

Article

Field Study and Multimethod Analysis of an EV Battery System Disassembly

Sonja Rosenberg ^{1,*}, Sandra Huster ¹, Sabri Baazouzi ² , Simon Glöser-Chahoud ¹ , Anwar Al Assadi ² and Frank Schultmann ¹ 

¹ Institute for Industrial Production (IIP), Karlsruhe Institute of Technology (KIT), Hertzstr. 16, 76187 Karlsruhe, Germany; sandra.huster@kit.edu (S.H.); simon.gloeser-chahoud@kit.edu (S.G.-C.); frank.schultmann@kit.edu (F.S.)

² Fraunhofer Institute for Manufacturing Engineering and Automation (IPA), Nobel Str. 12, 70569 Stuttgart, Germany; sabri.baazouzi@ipa.fraunhofer.de (S.B.); anwar.alassadi@ipa.fraunhofer.de (A.A.A.)

* Correspondence: sonja.rosenberg@kit.edu

Abstract: In the coming decades, the number of end-of-life (EoL) traction battery systems will increase sharply. The disassembly of the system to the battery module is necessary to recycle the battery modules or to be able to use them for further second-life applications. These different recovery paths are important pathways to archive a circular battery supply chain. So far, little knowledge about the disassembling of EoL batteries exists. Based on a disassembly experiment of a plug-in hybrid battery system, we present results regarding the battery set-up, including their fasteners, the necessary disassembly steps, and the sequence. Upon the experimental data, we assess the disassembly duration of the battery system under uncertainty with a fuzzy logic approach. The results indicate that a disassembling time of about 22 min is expected for the battery system in the field study if one worker conducts the process. An estimation for disassembling costs per battery system is performed for a plant in Germany. Depending on the plant capacity, the disassembling to battery module level is associated with costs between EUR 80 and 100 per battery system.

Keywords: disassembly; EV battery system; disassembly graph; fuzzy disassembly time; cost estimation



Citation: Rosenberg, S.; Huster, S.; Baazouzi, S.; Glöser-Chahoud, S.; Al Assadi, A.; Schultmann, F. Field Study and Multimethod Analysis of an EV Battery System Disassembly. *Energies* **2022**, *15*, 5324. <https://doi.org/10.3390/en15155324>

Academic Editor: Xiaoxiao Zhang

Received: 17 June 2022

Accepted: 20 July 2022

Published: 22 July 2022

Publisher's Note: MDPI stays neutral with regard to jurisdictional claims in published maps and institutional affiliations.



Copyright: © 2022 by the authors. Licensee MDPI, Basel, Switzerland. This article is an open access article distributed under the terms and conditions of the Creative Commons Attribution (CC BY) license (<https://creativecommons.org/licenses/by/4.0/>).

1. Introduction

Reducing the use of primary resources by developing an efficient and broad circular economy has been set as one cornerstone in the goals of the European Union to become climate neutral until 2050 [1,2]. The European Union has appointed the battery and vehicle value chain as one key market for implementing a circular economy [3]. As battery systems will power electric mobility in the upcoming years, they need to be at the center of attention to achieve the desired goals.

Circular economy options have been discussed intensively in the past years, i.e., the different pathways obsolete traction batteries might take. They can be divided into resource and product loops [4–9]. Resource loops are offered by recycling and can lower primary resource needs as recycled scarce resources are used as secondary material to produce new batteries.

Disassembling prepares an electric vehicle battery system (EVBS) to retrieve valuable resources. For recycling, such preparation may include a deep discharging of the EVBS followed by disassembling at least to a level where the battery modules are removed [10,11]. A further disassembling to cell level might be adjoined if special recycling processes are pursued [12,13]. As the disassembling of the EVBS for recycling does not focus on reusing the product or components, the disassembling may include destructive disassembling technologies. Today, manual disassembly is typical, and recyclers conduct it [14].

Before EVBSs or specific battery modules and cells are recycled, circular thinking asks whether repurposing, remanufacturing, or (partial) reuse are possible. Disassembly must preserve energy storage functionality in these cases, and deep discharging is impossible. Thus, the disassembling activities occur under high voltage conditions and require appropriate process safety measures [15]. They are often followed by reassembling activities.

In all cases of circular recovery processes, disassembling is mandatory for traction battery systems [5]. Some publications have addressed the disassembling of EVBSs in recent years and have documented the executed processes [10,16–19]. Besides that, other papers discuss requirements, potentials, and possible drawbacks for automatizing EVBS disassembling [5,20–22]. However, we find that only a little information can be gained from the documented disassembling experiments to estimate disassembling durations, which are needed to assess the disassembling cost of EVBSs. Additionally, the disassembling process is often only documented on an aggregated process level, and information about removed components or used fasteners is only partly available.

Thus, our paper pursues three goals. First, we document in detail the removed battery components, fasteners, and weights of the hybrid battery system under investigation. Secondly, we address disassembling durations from battery system to battery module level. We analyze and evaluate the measured durations by applying a fuzzy logic approach. The gained time information allows us to accomplish the third goal of estimating disassembling costs.

All three goals are important for different reasons. The disassembly costs can, for instance, be used together with retrieved material value to assess the economic potential of different treatment routes in a circular economy. Secondly, cost assessment of manual disassembling as conducted in industry and our experiment serves as a benchmark for economic profitability of automation. To develop efficient automation solutions, information about the disassembled product structure is crucial.

The structure of this paper follows the path of argumentation. Section 2 presents an overview of existing literature dealing with conducted disassembling experiments on electric vehicle (EV) battery systems and allows us to further distinguish our work from previous research. Section 3 explains which methods we use during disassembling and analysis. The structured results according to the applied methods form Section 4. Section 5 discusses our results before the paper is concluded in Section 6.

2. Literature and Research Gap

To point out how our approach differs from existing literature and highlight our contribution, we will present an overview of the most relevant literature for our research work, starting with conducted disassembling experiments of EVBSs in Table 1.

To our knowledge, the first available documentation of a manual EVBS disassembling is by [17]. They manually dismantled an Audi Q5 Hybrid battery system, which allowed them to elaborate a disassembling priority matrix and a disassembly priority graph. They use their results to conceptualize the design of a possible workstation in the content of a disassembly system. The authors of [17] neither address the topic of disassembly times nor costs, which we will further elaborate in our paper. A similar approach to [17] is presented by [16]. They show disassembling results of a VW Jetty Hybrid System, which seems equal to the Audi Q5 Hybrid battery system by [17] as their priority matrix and graph are identical.

Ref. [10] toto present an economic and ecological disassembly planning approach. The approach was applied to a case study on an Audi A3 Sportback e-tron Hybrid Li-Ion battery system. The documentation includes the main components and fasteners, their quantity, and a precedence diagram. The disassembly diagram and the explanation show that disassembly is mainly a serial process in which only two steps can take place in parallel. One of the two parallel steps is the disconnection of the high-voltage cables and the battery junction box. For calculating the disassembly costs, they refer to a Spanish remanufacturing plant. The disassembly costs are included in their economic and ecological

simulation model and are not reported explicitly. The authors of [18] are the only ones reporting on disassembly times for their manual dismantling of a Smart EQ Forfour battery system. The knowledge of the disassembly time is used for an economic calculation of the disassembly process. The reported cost is based on human labor and does not include capital expenditures, such as annual costs for a facility. The authors of [18] estimate that the disassembling from the battery system to module-level costs about 27 EUR/kWh and takes five hours for two workers.

Table 1. Literature with reported EV battery disassembly experiments and selected reported output data.

Source	Year	Vehicle/ Battery	Product Information	Disassembly Output	Disassembly Duration/Time	Disassembling Cost
[17]	2014	Audi Q5 Hybrid	Components	Priority Matrix; Disassembly graph process steps		
[16]	2019	VW Jetta Hybrid	Components	Priority Matrix; Disassembly graph process steps		
[10]	2020	Audi A3 Sportback e-tron Hybrid	Components and fasteners (quantities)	Disassembly graph process steps Disassembly Level		Costs are included in a simulation model; not given, e.g., based on disassembly time
[18]	2020	Smart EQ Forfour			Time in minutes for conducting process steps, e.g., cover removal	Costs for disassembly to module and cell level ¹ (only direct labor)
[19]	2021	2017 Chevy Bolt	Components and fasteners incl. specification; partly with weights and sizes	Disassembly graph incl. component specification		
This Paper	2022	PHEV 2018 midsize/large vehicle	Components and fasteners with information on quantities, screw types, sizes, material, etc.	Disassembly graph on compo- nent/component group level; Disassembly graph on detailed activity level ²	Measured disassembling durations for each activity ² Fuzzy Logic Approach to include uncertainty about real disassembling time for battery system and steps	Cost estimation for disassembly to module level • Scaling of results to medium- sized EVBS • Variable and fixed costs

¹ Further processing steps: Extraction of EVBS from vehicle and preparation for disassembly. ² Available in the Supplementary Material.

Apart from the studies in Table 1, few other authors have addressed the disassembling of EVBSs for related topics and have provided disassembling information. Ref. [23] used available data on an Audi A6 Hybrid Battery System to draw a product structure that constitutes a disassembling graph to depict the disassembling structure. Recently, ref. [24] developed a framework considering design, safety, and cost to evaluate the disassembly processes of generalized EV battery packs. They also assess improvements by disassembling with a partly automated working station. They do not conduct disassembling experiments but set up common steps based on the existing literature.

Disassembling costs are a potential barrier to the economic profitability of end-of-life (EoL) battery treatment [5,24,25], but only a few papers apply methods to calculate them. Papers [10,18] have already been listed in Table 1. Furthermore, ref. [25] calculated disassembling cost at EVBS level based on labor cost, the number of disassembling steps, and a

set duration per disassembling step. Their disassembling data are based on online information about different battery pack designs. The authors of [6] develop an optimization approach to determine the optimal disassembling strategy of EoL vehicle batteries, in which disassembling costs are included. Their cost calculation is based on [10,18], combined with information about average disassembling times in the industry of 30 min per EVBS with two workers.

Our paper contributes to the new research field of electric vehicle battery disassembling (see Table 1). We conducted a manual disassembling experiment of a hybrid electric vehicle battery system from the battery system to the module level. We present detailed information on disassembled components and fasteners. Although we merely describe sizes, weights, and materials (partly in the Supplementary Material S1), researchers can use this information for their needs, e.g., for validation purposes or as data input, when dealing with disassembly automatization, material flow analysis, or life cycle assessment.

We use our documented disassembling time data to calculate disassembling durations. Therefore, we present a calculation based on the critical path method (CPM) combined with fuzzy logic. We connect the results with a scheduling heuristic that considers limited available resources. Multiple scenarios of different workforce requirements are presented and discussed. The results are then employed to derive disassembling times for EVBSs of different weights with an upscaling method. Lastly, we perform a cost estimation for disassembling in Germany based on the previously won results. We extensively discuss the results in a comprehensive discussion section, which is also extended to disassembly automation to underline some implications of our findings.

3. Materials and Methods

3.1. Experimental Plan and Documentation

One of the goals of this paper is to give precise documentation of the disassembly process of an EVBS, more specifically, the EVBS of a Mercedes Plug-in Hybrid Electric Vehicle (PHEV) with 13.5 kWh. Therefore, we focus our experiment documentation on four aspects.

First, we want to provide a detailed description of the disassembly process. Existing publications dealing with EVBS disassembly describe the process on an aggregated level. We intend to fill the gap at the operational level by providing a detailed overview, including small activity steps such as unscrewing and removal. Identifying predecessors and successors of every activity allow for deriving a precedence graph.

Second, the duration required for each activity is recorded. This way, we can determine the time intensity of disassembling to a certain level. For example, one could aim to retrieve only the battery modules as components and therefore seek the fastest way to reach them. Then, one could add up the durations of the activities leading directly to the modules. On the other side, the duration to dismantle all parts, including the battery management control unit or fuses, could be determined. Knowledge of disassembly durations is crucial when developing business models for repurposing or remanufacturing, since these durations can influence the estimated profitability.

Third, details concerning the connections and disconnecting them are of interest. For each activity, we document the connection type, the orientation of the connection, and the tools needed for disconnection, if applicable. This information is required when assessing if a process can be automated and how complex it is. Although we do not discuss the potential of automation in this paper, this information can help other researchers with their work.

Fourth, information about the components resulting from each activity is obtained. This includes data on the component dimensions, their weight, and, if determinable, their material composition. These data can be used to plan automated disassembly processes and estimate the recyclability of the EVBS with and without disassembly.

Before the disassembling experiment, we studied information about the disassembling process and sequence recommended by the battery system producer. Thus, we knew which

tools were needed for each step and prepared the experiment set-up accordingly. Apart from the studied information, we did not have hands-on disassembling experience but a mechanical and business engineering background. The disassembled PHEV battery system was not an EoL product, but a de-energized system usually used to train manufacturing employees. The aim was to represent a disassembling working situation, where a disassembling is conducted based on information. Although it takes place manually, it represents a real-world working process, including the corresponding working speeds. It is worth mentioning that the disassembling started with the removal of the battery cover, and the disassembling stopped when all parts except the glued battery modules were removed. Removing the modules was impossible during the experiment because the needed tools were unavailable. However, this step has been conducted separately in another representative experiment with a PHEV system of the same type. Therefore, we rely on the document information of this second experiment for the battery module removing step.

3.2. Disassembling Duration Assessment by Fuzzy Logic

Uncertainty about accurate disassembling durations is one of many problems in disassembling planning. One reason for such uncertainty can be the not precisely known quality of EoL products that influence the disassembling duration [26,27].

According to [28], three methods and measures exist to model the uncertainty of disassembling times in mathematical problems. The disassembling duration can be modeled with a probability distribution [29], using interval numbers representing upper and lower bounds or fuzzy numbers [28]. We decided on applying a fuzzy logic approach because interval numbers can be transferred to a particular case of fuzzy numbers [30,31], and probability distributions cannot be specified with the available information.

The following steps describe the fuzzy assessment plan to determine the disassembling completion time and are described as comprehensively as possible in this section. Thus, if interest in fuzzy logic goes beyond the explanations in this section, we refer to Appendix A where deeper explanations, including further literature, are presented. A list of all used symbols and nomenclature is found at the end of the article.

1. Determine fuzzy durations for each disassembly step based on the conducted disassembling experiment and expert knowledge to validate the durations.
2. Conduct the critical path method (CPM), known for scheduling tasks with fuzzy durations to gain a feasible disassembling schedule with minimum total fuzzy disassembling time.
3. Apply a heuristic scheduling procedure with resource constraints to calculate the fuzzy and defuzzified disassembling times for different workforce settings.

In this paper, fuzzy disassembling durations are presented by the so-called six-point representation of fuzzy intervals (cf. Appendix A) [32], as illustrated by Equation (1). The six points allow a better representation of potential outliers than triangular or trapezoidal membership functions widely used in fuzzy modeling [33]. Meanwhile, they can also form triangular or trapezoidal membership functions, if applicable.

$$\tilde{D}_j = \left({}_o d_j^\varepsilon, {}_o d_j^\lambda, {}_o d_j^1, {}_p d_j^1, {}_p d_j^\lambda, {}_p d_j^\varepsilon \right) \quad (1)$$

For each fuzzy duration (\tilde{D}_j), a corresponding membership function exists (cf. Appendix A for definition) described by the six values. Figure 1 gives an explanatory illustration of such a membership function. The six values are based on estimations of lower and upper values for three membership levels ($\varepsilon, \lambda, 1$) (cf. Appendix A).

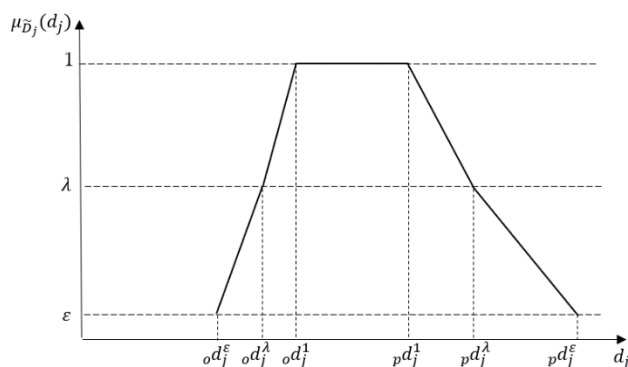


Figure 1. Illustrative example of a membership function based on six-point representation for a fuzzy disassembling duration D_j of process j (adapted from [26]).

We use the argumentation introduced by [34] to assess to which extent values belong to a fuzzy set (cf. Appendix A) represented by a corresponding membership function.

According to Equation (2), the value d_j belongs for sure to the values of fuzzy duration of disassembling process j if the membership function equals 1.

$$\mu_{\tilde{D}_j}(d_j) = 1 \tag{2}$$

Equation (3) means that a value d_j with $\mu_{\tilde{D}_j}(d_j) \geq \lambda$ has a fair chance of belonging to the group of fuzzy durations of process j .

$$\mu_{\tilde{D}_j}(d_j) \geq \lambda \tag{3}$$

Lastly, if Equation (4) applies, the value of d_j has only a very small possibility of belonging to the possible values of fuzzy durations of process j .

$$\mu_{\tilde{D}_j}(d_j) < \varepsilon \tag{4}$$

In practice and our use case, membership functions of disassembling steps are not known [35]. We model them based on several data sources representing optimistic and pessimistic values [36] for disassembling duration (cf. Section 4.2).

We specify how arithmetic operations are taken to perform calculations with fuzzy durations, each represented by six values in Table 2. The validity of the presented arithmetic operations is based on [37]. The subtraction \ominus is not an inversion of the addition, represented as \oplus . This may lead to wrong results in our calculations, and therefore, we apply the inverse addition \oplus^{inv} , when needed [26,38].

Table 2. Basic arithmetic operations of fuzzy numbers in six-point representation used for time calculations for two fuzzy numbers, representing fuzzy durations of process j and i [26,27].

Symbol	Arithmetic Operation in Six-Point Representation
$\tilde{D}_i \oplus \tilde{D}_j$	$(o d_i^\varepsilon + o d_j^\varepsilon, o d_i^\lambda + o d_j^\lambda, o d_i^1 + o d_j^1, p d_i^1 + p d_j^1, p d_i^\lambda + p d_j^\lambda, p d_i^\varepsilon + p d_j^\varepsilon)$
$\tilde{D}_i \ominus \tilde{D}_j$	$(o d_i^\varepsilon - p d_j^\varepsilon, o d_i^\lambda - p d_j^\lambda, o d_i^1 - p d_j^1, p d_i^1 - o d_j^1, p d_i^\lambda - o d_j^\lambda, p d_i^\varepsilon - o d_j^\varepsilon)$
$\tilde{D}_i \oplus^{inv} \tilde{D}_j$	$(o d_i^\varepsilon - o d_j^\varepsilon, o d_i^\lambda - o d_j^\lambda, o d_i^1 - o d_j^1, p d_i^1 - p d_j^1, p d_i^\lambda - p d_j^\lambda, p d_i^\varepsilon - p d_j^\varepsilon)$
$\widetilde{\max}(\tilde{D}_i, \tilde{D}_j)$	$(\max(o d_i^\varepsilon, o d_j^\varepsilon), \max(o d_i^\lambda, o d_j^\lambda), \max(o d_i^1, o d_j^1), \max(p d_i^1, p d_j^1), \max(p d_i^\lambda, p d_j^\lambda), \max(p d_i^\varepsilon, p d_j^\varepsilon))$
$\widetilde{\min}(\tilde{D}_i, \tilde{D}_j)$	$(\min(o d_i^\varepsilon, o d_j^\varepsilon), \min(o d_i^\lambda, o d_j^\lambda), \min(o d_i^1, o d_j^1), \min(p d_i^1, p d_j^1), \min(p d_i^\lambda, p d_j^\lambda), \min(p d_i^\varepsilon, p d_j^\varepsilon))$

Once the disassembling durations are determined for each step and the disassembling graph is set-up, the CPM can be applied. The critical path method is used in project

management to calculate time-related dates when planning a project. In our case, the disassembling process equals the project. The different disassembling steps need to be performed to fulfill the project goal of disassembling the battery system to module level.

We add a starting activity and an ending activity to our disassembling graph that both have durations of zero time units to represent a graph in network structure. This graph extension allows the application of the CPM. The starting activity is a direct predecessor of all steps that do not have successors, while it is the other way around for the ending activity.

During the calculation process to identify the critical path of a project, the total completion time of the project is determined, along with the earliest and latest starting and ending time of each activity [39]. The calculation steps to retrieve the starting and ending times are based on a forward and backward calculation theme and are described in detail in [39]. The fuzzy durations can be adopted as described in ref. [26].

The basic calculation steps for the forward calculation determine the activities' earliest starting and ending times. When calculating, the arithmetic operations given in Table 2 are obeyed for our six-point durations, as they are each a fuzzy number. The fuzzy earliest start (\widetilde{ES}) of the disassembling process is set to 0.

$$\widetilde{ES}_0 = (0, 0, 0, 0, 0, 0) \tag{5}$$

For all other steps j that have predecessors (i), the respective fuzzy earliest start (\widetilde{ES}_j) is given by

$$\widetilde{ES}_j = \max\{\widetilde{ES}_i \oplus \widetilde{D}_i \mid i \in P_j\} \quad \forall j = 1, \dots, J \tag{6}$$

Thus, a disassembling step j can only start if all predecessor activities are finished. The fuzzy earliest finish (\widetilde{EF}) for activity is given by

$$\widetilde{EF}_j = \widetilde{ES}_j \oplus \widetilde{D}_j \quad \forall j = 0, \dots, J. \tag{7}$$

The calculations of the backward procedure start with the last activity J , which has no successors. The fuzzy latest finish time (\widetilde{LF}) is set as the fuzzy earliest finish of activity J (\widetilde{EF}_J) as we do not have another external given the latest completion time for the project \widetilde{T} .

$$\widetilde{LF}_J = \widetilde{EF}_J = \widetilde{T} \tag{8}$$

All other disassembling steps (i) have at least one successor (j), and we apply the following:

$$\widetilde{LF}_i = \min\{\widetilde{LF}_j \oplus^{inv} \widetilde{D}_j \mid j \in S_i\} \quad \forall i = 0, \dots, J - 1 \tag{9}$$

The fuzzy latest start (\widetilde{LS}_j) can be received with

$$\widetilde{LS}_j = \widetilde{LF}_j \oplus^{inv} \widetilde{D}_j. \tag{10}$$

Fuzzy times can be defuzzified according to the principle of Equation (11). This defuzzification is built upon the argumentation for six-point representations by [40]. We apply the defuzzification scheme at different points of our calculation process to gain crisp numbers that allow us to compare and interpret different fuzzy durations or to use the crisp numbers for further actions, such as the cost estimation [41].

$$F(\widetilde{LF}_j) = \frac{1}{4(1-\varepsilon)} \cdot \left\{ (\lambda - \varepsilon) \cdot ({}_oLF_j^\varepsilon + {}_oLF_j^\lambda + {}_pLF_j^\lambda + {}_pLF_j^\varepsilon) + (1 - \lambda) \cdot ({}_oLF_j^\lambda + {}_oLF_j^1 + {}_pLF_j^1 + {}_pLF_j^\lambda) \right\} \tag{11}$$

Once the forward and backward calculations are conducted, we receive a feasible schedule for the disassembling process, with a minimum fuzzy project time that is equal to \widetilde{LF}_J .

The resulting schedule and fuzzy completion time can be reached if resources, primarily renewable resources, are sufficiently available or not limited. Potentially limited renewable resources in disassembly are the available number of workers, tools, or workspace. Therefore, including available renewable resources in calculating disassembling time is essential, as they can form a limiting factor that opposes the calculated minimum disassembly time.

We apply a widely adaptable scheduling heuristic, depicted in Figure 2, to include available resources in our disassembling schedule [26,32,42]. The pseudocode describes that whenever a new activity can start, all not yet scheduled disassembling steps that do not have unscheduled predecessors are looked at. From these groups of disassembling steps, the one with the highest priority is chosen to be conducted if enough resources are available. If there are insufficient resources for this activity, the next highest-ranked disassembling step from the priority list is considered. Meanwhile, the one with the highest priority is set aside for the next point of time when a new disassembling step can start. This planning procedure repeats until all disassembling steps are accomplished.

```

BEGIN
   $\bar{t} := \bar{t}_0, \Omega := \{\}$ 
REPEAT
  Compose a set  $Q(\bar{t})$  of those activities which have not been scheduled yet
  and whose immediate predecessors have been completed by time  $\bar{t}$ . Thus,
   $\bar{t}_i^f \ll \bar{t}, \forall i \in P_j \in Q(\bar{t}) \Leftrightarrow \overline{\max}(\bar{t}, \bar{t}_i^f) = \bar{t}$ 
  FOR each activity  $j (j \in Z)$  from  $Q(\bar{t})$ , in the order of the priority list DO
  IF  $j$ 's resource requirements  $\leq$  resource availabilities THEN
    IF  $\bar{a}_j \ll \bar{t} \Leftrightarrow \overline{\max}(\bar{a}_j, \bar{t}) = \bar{t}$  THEN
       $j$ 's start time:  $\bar{t}_j^s := \bar{t}$ 
       $j$ 's finish time:  $\bar{t}_j^f := \bar{t}_j^s \oplus \bar{D}_j$ 
      remove  $j$  from  $Q(\bar{t})$ 
      allocate required resources to  $j$ 
      insert  $\bar{t}_j^f$  into set  $\Omega$ 
    ELSE
      insert  $\bar{a}_j$  into set  $\Omega$ 
    END IF
  END IF
END FOR
 $\bar{t} := \overline{\max}(\bar{t}, \bar{l}) \Leftrightarrow \overline{\max}(\bar{t}, \bar{t}_i^f) = \bar{t}$ 
  IF  $\bar{l} = \bar{t}_j^f$  THEN
    update resource availabilities
  END IF
  remove  $\bar{l}$  from set  $\Omega$ 
UNTIL all activities from the priority list are completed.

```

with

\bar{t}	Current (fuzzy) time moment at which allocation of resources is considered to an activity
$\bar{t}_j^s (\bar{t}_j^f)$	Fuzzy Start Time (Fuzzy Finish Time)
\bar{l}	The least value from the set Ω , taking the defuzzified values
Ω	$\Omega = \{\bar{t}_j^f : \forall j \in S(\bar{t})\} \cup \{\bar{a}_j : \forall j \in A(\bar{t})\}$,
$S(\bar{t})$	The set of activities that have been scheduled before $\bar{t}, \bar{t}_j^s \ll \bar{t}$,
$A(\bar{t})$	The subset of $Q(\bar{t})$ of those activities that are not ready in moment $\bar{t}, \bar{a}_j \geq \bar{t}$.

Figure 2. Heuristic planning procedure for scheduling activities with fuzzy durations adapted from [26,43,44].

3.3. Cost Estimation

As discussed in Section 2, the cost estimation of EVBS disassembly has been addressed sparsely in previous works. Apart from [6,10,18,25], refs. [45,46] provide cost data for planning an EVBS disassembling center in Germany. Additionally, an often-cited cost model for battery recycling, the EverBatt Model, contains an estimation approach to evaluate disassembling costs [47]. The general approach used by [45,46] is identical. First, an investment sum is determined for a sufficiently sized factory, the required equipment, and ancillary cost. Based on the total investment sum, annual costs are calculated. Variable costs are associated with direct labor costs for disassembly.

From a broader literature perspective, disassembling costs are usually calculated as the variable cost needed to disassemble a product. According to refs. [48,49], two groups of methods for disassembling cost metrics are distinguished, namely technical and work measurement approaches. In technical approaches, disassembling durations are assigned to each step or movement depending on the fastener type. This disassembling duration is then multiplied by a cost factor of direct labor [50], which results in disassembling cost.

Work measurement approaches focus on evaluating factors, such as the accessibility of fasteners and how they influence a predefined and standardized duration for a specific disassembling action [51–57]. The evaluation results are scoring values that represent the difficulty of disassembly. These calculated values are then transferred into a disassembling time and costs [58,59]. Alternatively, a third possibility as input for cost calculations could be a direct measurement of disassembling time. Measurements should include the disassembly of several products of the same category by multiple workers with varying experience to result in representative results [54,60,61]. A repeated measurement can help measure uncertainty about the average of the expected disassembling time. The measured disassembling time is then multiplied by a disassembling cost that is assigned per disassembling time unit, comparable to the technical approaches. Fixed-cost components are barely addressed in general disassembly literature. Sometimes they are referred to as overhead costs and integrated by multiplying a factor to the variable costs [48,62].

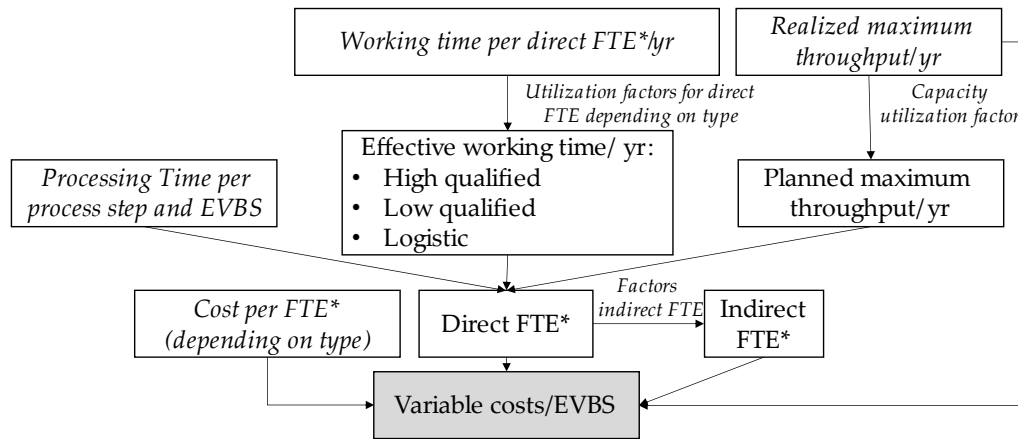
Before making a cost estimate based on the investments for an industrial disassembling plant, we need to transfer the results of the fuzzy disassembling duration approach to resemble an EoL battery system from a battery electric vehicle (BEV). This is necessary as we want to estimate the average disassembling costs of EVBSs. The PHEV battery system size will not be representative because the market share of EoL BEVs will be far larger [63].

The results transfer is conducted by upscaling the disassembling duration. We qualitatively and quantitatively evaluate how the fuzzy durations of each disassembling step deviate for battery systems from BEVs. This evaluation results in fuzzy disassembling durations for each disassembling step of a BEV. Once the fuzzy BEV disassembling durations are specified, we repeat the planning procedure explained in Section 3.2 to estimate a defuzzified complete disassembling time, which is input for the disassembly cost estimation as preparation for recycling.

Figure 3 highlights the conducted cost calculation schemes. The modeled plant processes are summarized in Figure 3a and consist of inbound logistics, storage, deep-discharging, disassembly, and logistical outbound processes. Figure 3b,c summarize the main steps of cost calculation. Founded on a disassembling capacity per year, we determine the variable cost for disassembly, constituted of labor costs. These labor costs include direct workers needed for disassembly and logistical processes and indirect labor, such as office workers. Although indirect employees are sometimes considered to be fixed costs, we include them in our variable costs.

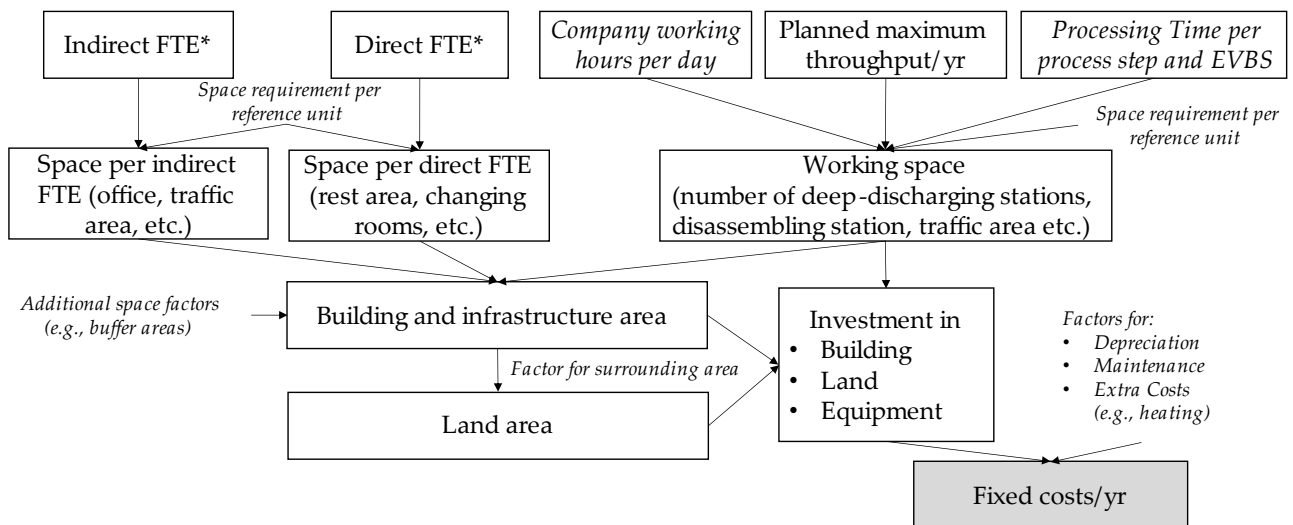


(a) Process stream in plant



(b) Calculation scheme variable costs per EVBS

*FTE = Fulltime Employee



(c) Calculation scheme fixed costs per year

*FTE = Fulltime Employee

Figure 3. (a). Modeled process stream of the disassembly plant; (b) calculation scheme for variable disassembling costs; (c) calculation scheme annual fixed disassembling costs; explanation for (b,c) cursive text indicates that the factor is an external input for calculation.

The fixed costs (cf. Figure 3c) can be divided into costs related to the factory’s property, building, and equipment. The total investment depends on the size of the factory, that is, depending on the planned throughput. We size the factory with a block structure approach, in which we calculate how much area is needed for each process of the value stream [64]. Therefore, such blocks may represent space for disassembling stations at which the disassembling takes place, a warehouse in which not yet disassembled EVBSs are stored, or the office space for an indirect worker. Such approaches are also founded in related literature [45,47]. The investment is used to receive the annual fixed costs, including different categories, such as depreciation and maintenance costs for equipment and imputed interests.

To give a realistic cost estimation, we take the use case of establishing a disassembling plant as preparation for recycling in Germany. Therefore, all cost components are fitted to resemble expected costs in Germany. Supplementary Material S2 provides detailed information about estimating single cost calculation steps and necessary assumptions. Therefore, in Section 4.3, we merely present the resulting cost structures.

4. Results

4.1. Disassembling Results from Experiment

As described in Section 3.1, we aimed to retrieve information about the process steps, including their duration, the types of connections that needed to be detached, and the retrieved components.

The disassembled PHEV battery system and the main components are shown in Figure 4 and Table 3. Figure 4 does not show all components but only those that need to be disassembled to retrieve the battery modules. The disassembly process begins with the removal of 40 screws and four clamping bars (A, B, C, and D). Then, the housing seal is cut, and the cover (E) is removed. The module block (K) consists of two modules that are screwed together. The modules are glued to the base using strips required for heat conduction and attached to the harness with four plugs and four cable clamps. In addition, they are fixed to the bottom of the housing with eight screws (four on the left and four on the right). The screws on the right side are accessible after disassembling the support strut (F) and the bus bar 1 with an integrated battery sensor (G). For this purpose, six screws, one plug, and two clamps must be removed (cf. Figure 3). The four screws on the left side can be unscrewed after removing the battery sensor (H), bus bar 2 (I), and bus bar 3 with an integrated fuse (J). The connections that need to be loosened are six screws, four plugs, and three clamps. In Appendix B, we provide some detailed information about the location of the individual screws and the center of gravity of the components on a xy-coordinate scale (cf. Figure A1). In Supplementary Information S1, a list of these coordinates is given.

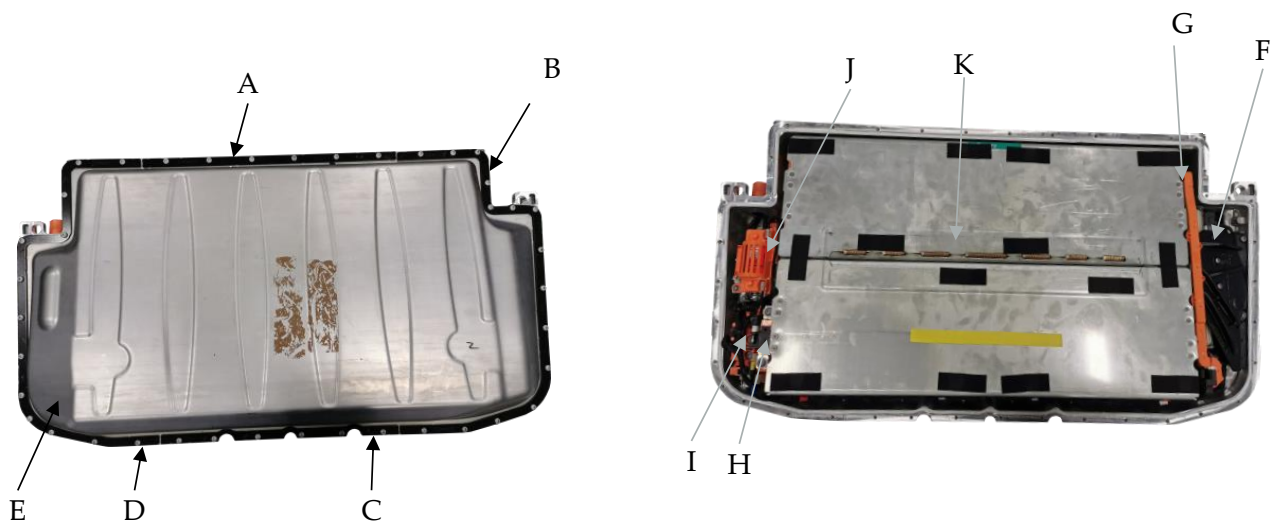
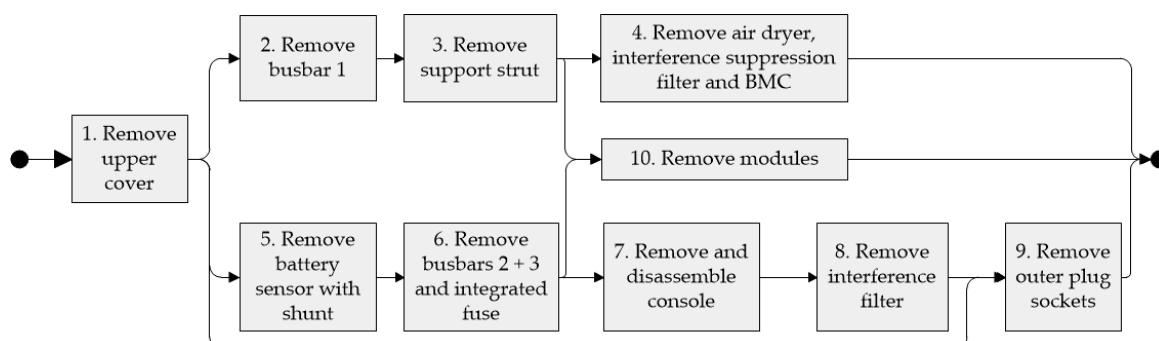


Figure 4. Picture of the disassembled PHEV battery system: A—clamping bar 1, B—clamping bar 2, C—clamping bar 3, D—clamping bar 4, E—cover, F—bus bar 1 (with integrated battery sensor), G—support strut, H—battery sensor (with shunt), I—bus bar 2, J—bus bar 3 (with integrated fuse), K—module block.

Table 3. Battery parts and connections. The IDs for the different components refer to Figure 4.

Parts	ID	Connections
Clamping bar 1	A	6 screws
Clamping bar 2	B	15 screws
Clamping bar 3	C	6 screws
Clamping bar 4	D	13 screws
Cover	E	1 glue 2 screws
Bus bar 1	F	1 plug 2 clamps
Support strut	G	4 screws
Battery sensor	H	2 screws 1 plug
Bus bar 2	I	2 screws 1 plug 4 screws
Bus bar 3 with integrated fuse	J	2 plugs 3 clamps 8 screws
Module block	K	4 plugs 4 clamps
Remaining parts	-	-

We identified 57 sub-steps to disassemble the PHEV and each component as far as possible in the experiment to module level. These 57 steps all have predecessor and successor relationships so that a detailed disassembly graph can be derived (see Supplementary Material S1). There are logical groups among the process steps belonging to one component or assembly. For example, multiple steps are necessary to remove the battery cover or the battery sensor. These related steps must be performed in spatial closeness to each other, so it seems reasonable to group them into top-level steps, as depicted in Figure 5. While in other publications, battery disassembly is described as a predominantly linear process (e.g., [10]), our battery allows parallelization of several dismantling steps. This is mainly because the battery periphery (e.g., interference suppression filter, BMC, battery sensor, fuse, etc.) is located at two ends of the battery, so it is possible to work on both sides simultaneously and to a certain degree, independently. Specifically, steps 2, 3, and 4 are located on one side of the battery, and steps 5, 6, 7, 8, and 9 are on the other (cf. Figure 5). It should be noted, however, that the battery's outer dimensions of about $0.90 \times 0.48 \times 0.21$ m (length \times width \times height) limit the possibilities of process step parallelization to a maximum of two workers.

**Figure 5.** Disassembly graph (shortened).

Besides the precedence relations, Figure 5 also reveals that not all process steps are necessary to perform when only aiming at retrieving the modules. The modules can be reached if steps 1, 2, 3, 5, and 6 are completed. All other steps (4, 7, 8, and 9) are optional but might be sensible when the corresponding parts shall be reused or a better pre-sorting of materials for material recovery is desired.

A more detailed description of the ten top-level process steps can be found in the Supplementary Material S1. There, each sub-process is described verbally (e.g., “Remove screws from cables (2 pcs)”), the average duration is given, and the required tools are indicated. Figure 6 shows an extract of the detailed disassembly graph using the example of step 8, “Remove interference filter”. This process is representative since it contains all three sub-processes that mainly form the top-level processes, i.e., the removal of screws with a screwdriver, the opening of plugs with pointed pliers, and the removal of unfastened parts by hand.

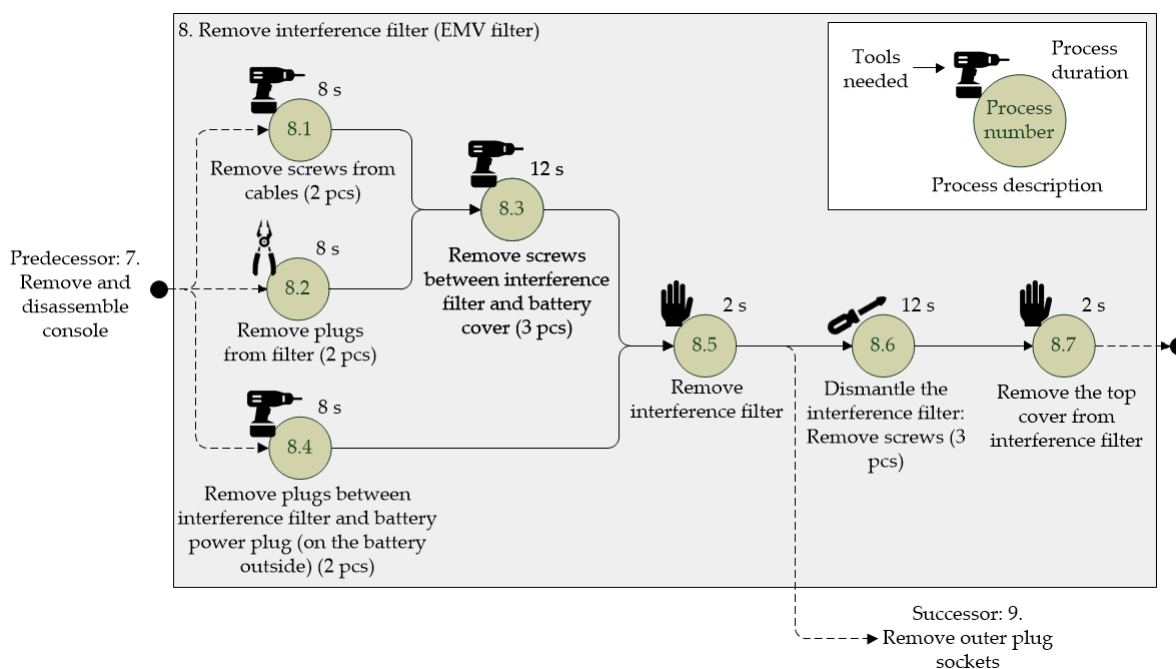


Figure 6. Detailed process description using the example “8. Remove interference filter”.

As mentioned in Section 1, disassembly is a necessary preparational step for several EoL options, e.g., remanufacturing, repurposing, or recycling. To not exclude options containing the reuse of the whole battery or components, we tried to unfasten all connections non-destructively so that reassembling would be possible. Most connections are either screw or plug connections. A (cordless) screwdriver can unfasten the screw connections with only a few bit changes. Most of the screw heads are inner-torx (bits: T20, T25, T30), and only the modules are fastened by outer-torx screws (bit: E10), and the high-voltage plug socket with hexagon socket screws (bit: V3). Besides that, an extension for the cordless screwdriver is necessary to reach some screws that are difficult to access. On average, it takes about four seconds to unfasten a screw. This is in line with the literature. The authors of [65], for example, measure 2.4 s to unfasten a screw excluding the time for motion (to and from the screw); those of [49] estimate 1.1 to 2.2 s for short screws, also excluding time for motion; and those of [66] specify a standard disassembly time of 6.5 s per screw.

Snap-fit fasteners mainly require pointed pliers to open them, partially damaging the plugs, as nearly all of them are also fixed with a latch. That indicates that the snap-fit fasteners are not designed for multiple-use cycles. In our case, it took 4 to 14 s to open one snap-fit connection. Other publications indicate this type of connection to be disconnected faster [49,65]. However, the complexity of unfasten snap-fits depends on the beam length, the retention angle, and the number of concurrent snaps [67]. We suspect that the retention angles of our battery’s fasteners are relatively large (>60 degrees), so they are well-secured and somewhat difficult to open. This aligns with the literature values of 7.5 s per complicated click-connection [66].

To remove the top cover, a cutter and something to lever, e.g., a manual screwdriver, are necessary as the cover is fastened with 40 screws and glue that needs to be cut. A levering

device prevents the cut parts from making contact and sticking together again. Besides the already mentioned tools, we needed a wrench to loosen a nut and adhesive tape to secure the pole cap covers. An overview of the required tools is given in Appendix B.

The retrieved main components are listed in Table 4. We refer to the Supplementary Material S1 for a more detailed examination of the components, their measures, weights, and materials at the screws and nuts level as well as the needed tools for disassembly.

Table 4. Retrieved components and some of their corresponding properties.

Main Components	Measures [mm]	Weight [g]	Materials
Upper cover	900 × 480 × 100	3690	Steel
Housing base	898 × 480 × 180	unknown	Steel
Busbars (3)	380 × 20 × 15	256 + 66 + 217	Metal core, coated with plastic
Support strut	230 × 150 × 20	1252.5	Steel
Air dryer	225 × 14 × 27	594	Plastic and silicate
Interference suppression filter	135 × 60 × 20	153	Plastic and cables
BMC	190 × 105 × 25	343	Plastic housing, circuit board
Battery sensor	95 × 45 × 15	47	Steel, copper, plastic
Fuse	92 × 31 × 31	138	Metal
Console	140 × 110 × 60	1284	Mixed
Interference filter	120 × 73 × 107	882	Mixed
Outer plugs	43 × 45 × 43 (excluding cables)	59	Plastic and cables
	50 × 65 × 35	141	Steel
Modules	610 × 398 × 185	136,000	Mixed
Rest	-	approx. 2700 (1300 for screws, nuts, and clamping bars)	Mixed

4.2. Disassembling Duration Assessment by Fuzzy Logic

As described in Section 3.2, we apply a combination of the CPM and fuzzy logic for the disassembling durations to calculate the needed disassembling duration. To conduct a time planning with the CPM, we use the precedence graph presented in Figure 5 and add so-called start and end tasks with durations of 0 s (dummy activities). We only consider the main disassembling steps of this shortened graph, thus adding up single activities within these steps. This decision was taken as the disassembling execution showed that due to the spatial closeness of the battery, it would not be possible to perform them in parallel during a manual disassembly.

Before conducting the calculations, the fuzzy durations were determined based on knowledge gained during disassembling, expert knowledge, and documented literature on different, representative disassembling tasks and movements [51,52,65]. The membership levels were defined before assessing disassembling durations were conducted on activity level.

In Section 3.2, we introduced the used six-point representation. The six points allow modeling the potential deviation of disassembly duration more precisely than a more common triangular function. The membership level ε was set to 0.1, and λ is equal to 0.6 in our calculations, as they can also be found in [32,36,68]. These levels, together with the level of 1, form the possible breakpoints of the membership function (cf. Figure 1). Using the level of $\varepsilon = 0.1$ permits some very optimistic or pessimistic durations that are not included in the assessment. During the assessment, some tests were performed to ensure that a slight variation of the membership levels λ and ε does not significantly change the defuzzified durations.

Although unique, the described activities in Section 4.1 include many repeated activities: Unscrewing, removal by hand, and releasing snap-fit fasteners with latches. The unscrewing showed only low time variations, and most of the screws were of the same type (cf. Section 4.1). We placed four seconds in the very likely regions, according to the argumentation in Section 4.1. The upper limit for the likely value group is five seconds, and

we further set symmetrical values for the ε , λ , -levels. Thus, the six-point representation for unscrewing one single screw is given as

$$\widetilde{D}_{screw} = (3, 3.5, 4, 5, 5.5, 6). \quad (12)$$

Such a time evaluation was done for each sub-activity of the disassembling process. Although each activity is looked at individually, for the “removal by hand” and “releasing a snap-fit” activities, we used the time representations in Equations (13) and (14). Releasing snap-fits with latches is generally associated with an asymmetrical fuzzy duration. The resulting piecewise linear function has a right tail. Meanwhile, the “removal by hand” activities could also be represented by a triangular representation, as the optimistic and pessimistic value for the α - levels $\alpha_1 = 1$ are equal.

$$\widetilde{D}_{hand} = (1, 1.5, 2, 2, 2.5, 3) \quad (13)$$

$$\widetilde{D}_{snap} = (4, 6, 7, 8, 9, 14) \quad (14)$$

In Appendix C, we provide a table with the six-point fuzzy durations of each subtask (cf. Table A1). Not all activities can be described with these three general fuzzy durations (Equations (12)–(14)). Therefore, further explanations are included. Some snap-fit or other plug removals were also calculated with addition of or reduction in time to Equation (14), depending on their accessibility, which is a common approach in estimating disassembly times [52,53]. As explained above, we assume that each task within a disassembly step is conducted in series. Therefore, we add up the durations of activities based on the addition rule in Table 2 and retrieve the fuzzy durations in Table 5.

Table 5. Derived fuzzy durations for main disassembling steps in six-point representation.

Step j	Description	Duration [s] $\widetilde{D}_j = (\dots)$
0	Start	(0, 0, 0, 0, 0, 0)
1	Remove upper cover	(349, 461, 508, 615, 680, 737)
2	Remove bus bar 1	(25, 36.5, 42, 54.5, 59.5, 77)
3	Remove support strut	(13, 15.5, 18, 22.5, 24.5, 27)
4	Remove air dryer etc.	(138.5, 182.5, 213.5, 254.5, 285.5, 365.5)
5	Remove battery sensor	(27.5, 34, 39.5, 48.5, 54, 63.5)
6	Remove bus bar 2+3 and integrated fuse	(31, 37.5, 44, 53, 59.5, 66)
7	Remove and disassemble console	(80, 108.5, 128, 154, 173.5, 229)
8	Remove interference filter	(36, 49, 58, 70, 79, 104)
9	Remove outer plug sockets	(16, 20, 24, 28, 32, 36)
10	Remove modules	(93, 107, 127, 152, 142, 186)
11	End	(0, 0, 0, 0, 0, 0)

The fuzzy durations in Table 5 are used to calculate the fuzzy latest finish time for each step (\widetilde{LF}_j) (cf. Table A2). We apply Equation (11) to determine the defuzzified latest finish of each step ($F(\widetilde{LF}_j)$), which is presented in Table 6. The defuzzified latest finish of each step ($F(\widetilde{LF}_j)$) is used to assign priority numbers that are then used in the scheduling procedure (cf. Table A3).

Table 6. Defuzzified latest finish time of disassembling steps.

Step j	Defuzzified Latest Finish Time $F(\tilde{LF}_j)$ [s]	Priority Number Based on $F(\tilde{LF}_j)$ (1: Highest Priority)
0	0	1
1	560.64	2
2	631.39	4
3	631.39	5
4	889.97	8
5	605.06	3
6	653.56	6
7	798.31	7
8	889.97	9 *
9	889.97	10 *
10	889.97	11 *
11	889.97	12 *

* If multiple $F(\tilde{LF}_j)$ are equal, numbering according to step order in disassembling graph.

The parallel planning heuristic includes limited renewable resources during the scheduling and time calculations. Different things can be a renewable resource in scheduling, such as a limited number of machines, tools, or the number of available workers. In our case, we consider only workers to be such resources. Each worker is equipped with a cordless screwdriver and other needed tools. The only fixed installed tool required is the lifter to remove the battery modules. Because only one activity needs this resource, it will not form a resource that can become a bottleneck.

The planning procedure is conducted several times. Only one worker is available in the base scenario, and all steps must be conducted (name: “One worker” or Scenario 1). Two workers are available for the disassembly in the second scenario, and each step can only be conducted by one worker (name: “Two workers” or Scenario 2). As the battery cover’s physical dimensions allow the unscrewing with two workers in parallel, we create a third scenario (name: “Two workers, cover together” or Scenario 3).

We summarize in Tables A4–A6. the fuzzy earliest and latest times of all steps for the different scenarios in Appendix C. The fuzzy durations can also be illustrated as fuzzy Gantt diagrams, which can be found in Figures A2–A4. As we are primarily interested in the total fuzzy disassembling duration of the different scenarios, we use Figure 7, which contains the membership function of fuzzy disassembling completion time, for further argumentation. As explained above, the degree of membership for the membership levels was set in advance before estimating the fuzzy disassembling durations of the steps. The course of the lines for the scenarios results from our fuzzy heuristic approach.

The graph in Figure 7 can be interpreted according to the definitions of fuzzy logic taken in Section 3.2. In our base case, the “One worker” solution, the disassembling process will most likely take 20 to 24 min (1202–1449 s). In the most optimistic situation, that is not very likely, disassembling takes about 13.5 min. In the pessimistic but just as unlikely case, it takes 31.5 min. The fuzzy disassembling time can also be defuzzified with Equation (11), leading to 22.2 min (1331 s). The defuzzified completion time of the “One worker” case is over 30% longer than that calculated with CPM (cf. Table 5), as no parallel processes can occur.

If two workers are available, the defuzzified disassembling time is about 16 min. In contrast to the “One worker” case, the duration is shortened as expected but cannot be cut in half. Only one of two workers is scheduled during the cover removal, while the other has idle time. The third scenario, “Two workers, cover together,” has a defuzzified time of about 720 s or 12 min.

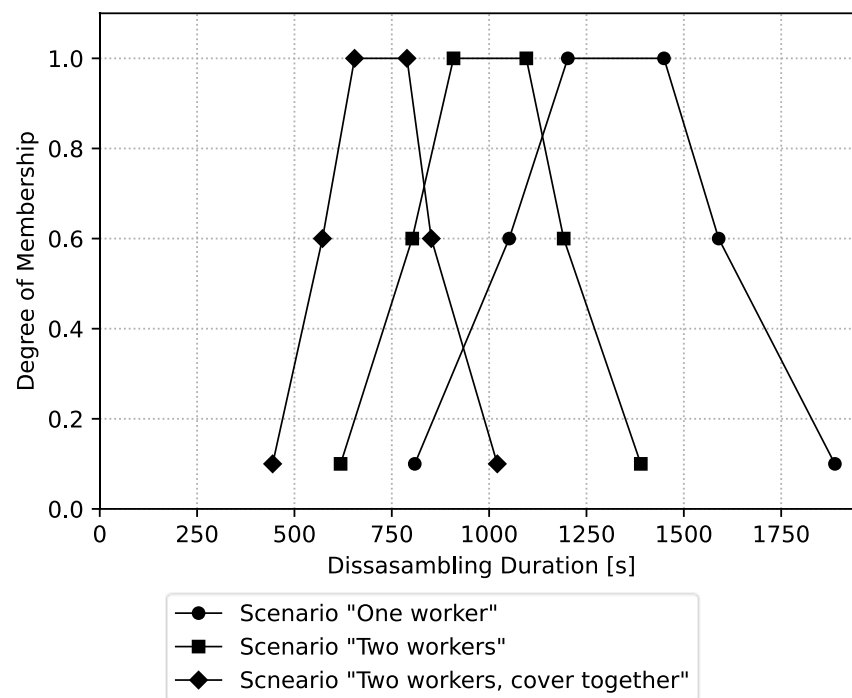


Figure 7. Membership function of fuzzy minimum disassembling completion time for different planning scenarios.

In the scenarios with two workers, step nine, removing outer plug sockets, is partially parallel to removing the module that is conducted with a lifter. Although from a precedence perspective possible, these two steps would most likely not be conducted simultaneously due to safety measurements in industrial practice. Thus, the total fuzzy disassembling completion time would likely be longer by the fuzzy duration of step nine. However, time savings could be credited during the removal of the modules, as some sub-steps might be conducted in parallel.

As stated in Section 4.1, we conducted a reversible disassembling of each step whenever possible. Therefore, we solved all snap-fit and press connectors by hand, which allows us to put them back together, which is required if a reassembling is planned, for instance, during a remanufacturing process. Nevertheless, if the aim is to recycle the battery, different disassembling techniques that save time but are not reversible might be applied. Determining the best tool and technique for each disassembling step requires intensive knowledge and experimentation time and did not occur during our disassembling experiment. Nevertheless, we want to demonstrate which disassembling duration differences are expected if snap-fit connections and their corresponding cables are cut with a knife or wire cutters [24] instead of releasing them carefully. Therefore, we change the general fuzzy snap-fit removal duration given in Equation (13) to the fuzzy duration of “removal by hand” given by Equation (12) and repeat all necessary calculations. As before, not all durations for cutting activities are equal in our calculation but can have added time if they are not well accessible.

Table 7 summarizes the shorter defuzzified disassembling completion time for the three scenarios discussed before and records possible time reduction between 11.3% and 19% if cutting is applied. This significant difference in duration confirms the assumption that requirements on the disassembling output, such as the possibility of reusing parts for reassembly, can influence the disassembly time.

Table 7. Comparison of defuzzified disassembling completion time for different scenarios and plug removal techniques.

Scenario Name	Defuzzified Disassembling Completion Time [min]		Reduction in %
	Conducted	Alternative	
One worker	22.2	18	19
Two workers	16.7	15	11.3
Two workers, cover together	12	10.3	16.5

4.3. Cost Estimation

Section 3.3 describes that cost calculations for disassembly processes are based on disassembling times. It must be questioned what a representative disassembling time and product for this cost is. As we wish to perform a rather wide-range cost estimation of disassembling EVBSs, we need to determine the disassembling time of an average EVBS. Our used PHEV battery system is relatively small in size, weight, and capacity compared to EVBSs employed in BEVs [5,69]. Therefore, we wish to scale the expected disassembling time to represent EVBSs used in purely electric battery vehicles. There are no guidelines in the literature to scale disassembly times without having specific information about the different sized products. The findings of [61] on disassembly times for TVs and monitors indicate that the disassembly time increases disproportionately low with the mass and size of the product, although the authors also find significant time variances for monitors and TVs with the same mass or size specification. The authors of [70] report on an increasing disassembling time depending on the type and number of fasteners, which aligns with the technical approaches discussed in Section 3.3.

Although not a technical approach, our fuzzy disassembling time approach in Sections 3.2 and 4.2 is based on the type and number of fasteners. Therefore, we evaluate how an increase in battery size, represented by the battery module weight, changes the expected fuzzy disassembling time if the battery design is kept.

We first conduct a qualitative evaluation to determine if the duration of a single disassembly step increases proportionally to the battery module weight. Therefore, we use information gained from available online videos of disassembling processes for over 15 different PHEVs and BEVs (cf. Supplementary Material S3). Table 8 presents the results of this first qualitative evaluation. The evaluation was performed separately for each disassembling step, and for some steps, we wish to point out our argumentation.

Table 8. Evaluation of proportional influence on disassembling time with increasing EVBS battery module weight.

Step j	Description of Step	Proportionality	Beta Value (for Equation (15))
1	Remove upper cover	↓	[0.6; 0.7; 0.8; 0.9]
2	Remove bus bar 1	→	1
3	Remove support strut	→	1
4	Remove air dryer etc.	↓	0.7
5	Remove battery sensor	↓	0.7
6	Remove bus bar 2 + 3 and integrated fuse	→	1
7	Remove and disassemble console	↓	0.7
8	Remove interference filter	↓	0.7
9	Remove outer plug sockets	↓	0
10	Remove modules	→	1

Symbology: ↓ lower increase, ↑ higher increase, → proportional.

With an increase in module weight, the battery's frame size increases. However, this increase will be disproportionately low due to the relationship between the perimeter and surface of the battery system. The frame size can be interpreted as a proxy variable for

the needed number of screws. The step “remove outer plug sockets” can be considered independent of the battery module weight. An assumption of our evaluation is that number of contained battery modules increases. We set the step “remove modules” to be proportional to the battery weight, as not all modules can be removed together. Instead, the module removal occurs after another (cf. Supplementary Material S3). The same argumentation comes into place for the bus bars and support strut.

The quantitative assessment is based on the expected proportionality for each disassembling step. We assume that a fuzzy disassembling duration follows a scaling as

$$\tilde{D}_{j^{new}} = \tilde{D}_{j^{org}} \cdot \left(\frac{Bat^{new}}{Bat^{org}} \right)^{\beta} \cdot \gamma. \quad (15)$$

The parameter of battery module weight (*Bat*) is chosen as a reference point for qualitative upscaling. We do not choose energy capacity as a reference, although it is common to present cost in relation to a battery capacity (EUR/kWh). Analyzing the specific energy (kWh/kg) of BEVs and PHEVs shows a significant disparity due to different power and energy requirements for the battery cells in the vehicle [71]. In contrast, the battery cell weight/kg battery pack is less varying [71] and, therefore, seems to fit better. We use the weight of the battery modules as we did not disassemble the modules and, therefore, do not fully know the cell weight.

The value of β , the exponential scaling factor, was not derived mathematically but is based on the qualitative proportionality evaluation. Table 8 contains the applied beta values for each disassembling step in the right column. The γ -term allows us to include additional disassembling time changes that are not related proportionally to the battery module weight and the corresponding β -values. In Equation (15), each fuzzy duration is multiplied by a crisp number, resulting in a new fuzzy duration. This allows us to repeat the planning procedures explained in Section 4.2 with the scaled fuzzy durations.

Figure 8 illustrates how the disassembling duration is expected to vary depending on the EVBS module weight, workforce settings, and different beta and gamma values for the “cover removal” step. As expected, the defuzzified disassembling duration increases disproportionately low with an increase in total battery module weight. Doubling the battery module weight will increase the disassembling duration between 63% and 78% (beta cover removal 0.6–0.9 and gamma 1). An EVBS with a 375 kg module weight is estimated to have a disassembly duration of between 48 and 59 min.

We decided to use a disassembling time of 53 min for one worker and 30 min for two workers as input for the cost calculation, which corresponds to a battery module weight of 375 kg, a beta value for cover removal of 0.8, and a gamma of one. We estimate the total costs divided into fixed and variable costs according to the presented scheme in Figure 3 for different capacity sizes of disassembling plants in Germany.

Figure 9 presents the cost estimation results for selected throughput classes in units of disassembled battery systems per year. The total cost per EVBS, including fixed and variable costs, declines with increasing capacity sizes of the plant and is between 80 and 110 EUR/EVBS. The variable costs show a slight variation, depending on the utilization of the required full-time employees. The variable costs for the smallest capacity size of 5000 EVBS/year are lower than in the case of 10,000 EVBS/year. One reason is that no employees are needed for management tasks associated with high wages for the smaller capacity size. For the larger capacitated plants, the share of indirect work per battery declines as the personnel is used more efficiently. Comparing the costs for the calculation with different workforce settlements shows that the fixed costs associated with disassembly stations do not make up a significant share. The larger part of fixed costs is associated with different areas needed for logistical processes that are identical to the different workforce scenarios. In all cases, the variable costs are higher if two workers disassemble the EVBSs together due to the disassembling times of 53 and 30 min.

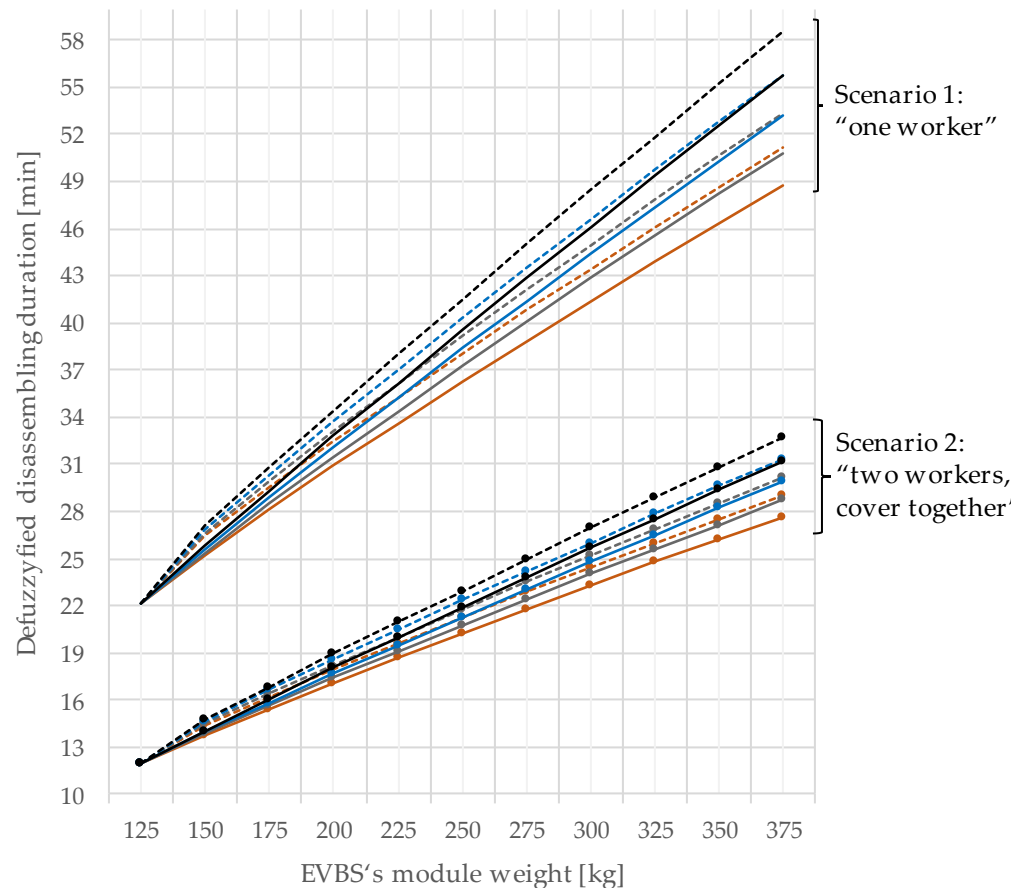
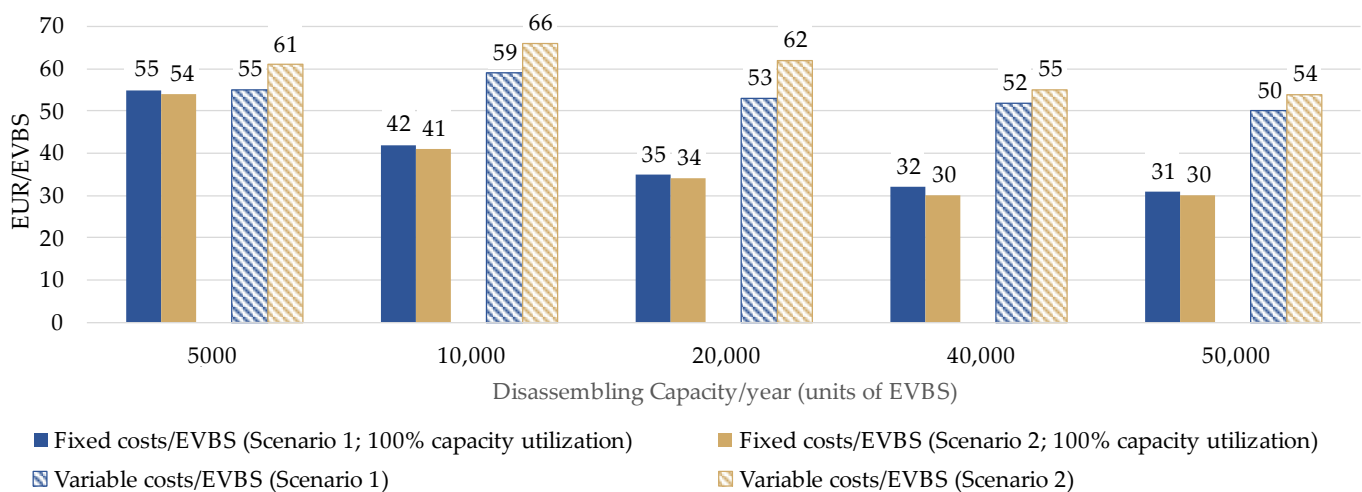


Figure 8. Defuzzified disassembling durations depending on EVBS modules' weight, workforce settings, and scaling parameters for cover removal; line colors represent different beta values for "cover removal" step: brown 0.6, grey: 0.7, blue 0.8, black 0.9; type of line represents gamma: solid: $\gamma = 1$; dashed: $\gamma = 1.05$.



EVBS: electric vehiclebattery system

Figure 9. Variable and fixed costs per EVBS for different disassembling plant sizes in Germany.

5. Discussion

As our conducted multimethod analysis allows us to discuss various aspects, we structured this section according to the applied methods. We added a further subsection to discuss the adjacent topic of disassembly automation.

5.1. Disassembling Results from Experiment

Many factors influence the results of the disassembling experiments. Among them are the experiment setup and the architecture of the examined EVBS.

The experiment setup was characterized by its local surroundings, the people executing the disassembling, and the battery charging status. The disassembly side was a well-equipped laboratory but not specifically designed for battery dismantling. We prepared the place to have all tools by hand and excluded times for additional tool acquisition.

However, a workshop designed and equipped for EVBS dismantling could have provided better conditions with differing disassembly times. The same holds for the persons executing the disassembling. We have mechanical and industrial engineering backgrounds but are not trained mechanics. This might have influenced the disassembly times and tool choices.

Additionally, the experiment was conducted with an inactive battery. When disassembling an EVBS for the potential reuse of the whole system or single components, deep discharging of the battery is impossible, as this would permanently damage the battery cells [72]. Therefore, it would be inevitable to work on a charged high-voltage EVBS, which requires precautions [73] that could affect the disassembly time and the required tools. Further research could verify if the disassembly times and tooling choices we measured also apply in an industrial setting.

The battery architecture extensively affects the results. The measures and weights of components can especially differ significantly between EVBSs. This is partially considered in Section 4.3, where the effects of upscaling on the disassembly times of the components are examined. However, it is unclear if this covers architectural choices sufficiently, e.g., when more or fewer cells are grouped into one module. For instance, a Tesla Model S P85 battery pack contains 7104 cylindrical cells grouped into 16 modules [74], while the 77 kWh ID.3 battery comprises 288 pouch cells grouped into 12 modules [75]. The same holds for different joining technologies used in EVBSs [76].

Furthermore, while the main components are most likely contained in all batteries, others are optional. Our battery, for example, does not have an active cooling system, so we did not have to remove any potentially hazardous cooling liquid. Different kinds of connections and components might also influence the tool choices. Nevertheless, the results from our disassembling experiments concerning the time and tool requirements and the retrieved components can serve as a basis for analysis. Further empirical studies for comparison would be beneficial for the scientific community.

5.2. Disassembling Duration Assessment by Fuzzy Logic

We applied a fuzzy logic scheduling approach for the disassembling steps in combination with a critical path method commonly used in project management. To our knowledge, we are the first to use fuzzy logic to determine disassembling durations of an EV battery system (cf. Appendix A). One significant advantage of fuzzy logic is that it includes uncertainty, which is non-statistical. It allows us to include human factors, such as disassembling experience or the varying quality of an EoL product.

The derived fuzzy durations for each disassembling step are grounded on distinct sources, such as expert knowledge and literature. A comparison with other recorded disassembling experiments should be performed to verify to what extent our results are reasonable.

In Section 2, we explained that there is only one other disassembling experiment that reports disassembling durations. The authors of ref. [18] disassembled a Smart Forfour battery system with comparable weight and energy characteristics to our hybrid battery

system, though the components are not identical in amount, type, and design. They report a duration for dismantling to module level by two workers of 300 min, which is far higher than our defuzzified time of 12–16 min for two workers (cf. Table 7) or our most pessimistic time estimate of 24 min. In ref. [18], the cover is fixed with about double the number of joints (screws and nuts) compared to our battery. The reported disassembling time for the cover of 30 min with two workers is far higher than our defuzzified time of 9 min for one person. If we double our fuzzy duration to account for the double number of joints, our most pessimistic value comes to 24.5 min for one worker. Splitting this in half (cf. scenario “two workers, cover together”) to include two workers, as in ref. [18], yields about twelve minutes per worker in the most pessimistic time estimate. Thus, a considerable difference exists, especially since the Smart Forfour battery does not need intensive cutting of adhesive [18]. However, it should be noted that the authors of ref. [18] conducted their experiment on a non-deep-discharged battery under high voltage conditions.

Further statements about archived disassembling times for EVBSs can help to rationalize our results. As mentioned in Section 2, ref. [6] reports on average industry disassembling duration of 30 min for two workers. In ref. [77], a disassembling time of 20 to 60 min depending on the EVBS is reported. Ref. [78] reports a disassembling duration of 25 min. Ref. [79] calculates with a disassembling duration of 0.7 h in their economic evaluation and report that this value is based on a disassembling execution for a BMW i3 battery system. Although we cannot verify our results with this literature information, as there is no detailed information about the size and type of EVBS, they underline that our results are reasonable.

We conducted the scheduling heuristic for different scenarios to receive alternative fuzzy and defuzzified disassembling times. As it is a heuristic, the solution is not guaranteed to be optimal. However, it yields good results with little effort to solve the scheduling tasks and is comparable to the thinking and planning of a disassembling process, as it is conducted in practice [61] when an optimal schedule for the given resource setting is not known.

The optimality of a disassembling schedule, i.e., the sequence, could be proven by setting up and solving an optimization model for a corresponding resource constrained scheduling problem [80,81]. Indeed, we know that the planning with the scenario of one worker is optimal, as the fuzzy completion time is equal to the sum of the fuzzy durations for the steps. The authors of [82] point out that disassembling scheduling with uncertain parameters has barely been addressed in the literature. Thus, even a heuristic scheduling procedure can extend the method and add new value.

First insights were given that the sought usage options for components after disassembling influence the disassembling time significantly. This resembles the fact that remanufacturing might come with different disassembling processes from recycling. Especially for remanufacturing and repairing, selective disassembling has to be addressed [83]. A selective disassembling may also be of interest if only selected parts must be retrieved, such as the battery modules and the BMC. Although containing different materials, other components may be processed in mechanical disassembling steps such as shredders [61]. In these cases, knowledge about the alternative disassembling times is needed for an economic trade-off calculation.

5.3. Cost Estimation

The results of our cost estimation indicate that variable as well as fixed costs are equally important when dealing with the total cost of disassembly. The calculated disassembly costs are higher than one would associate when only considering the variable labor cost of the disassembly workers [84]. EoL EVBs are dangerous goods, and due to their large dimensions and weights, higher logistic costs than for other waste products are expected in EVBS disassembly plants. In contrast to many other EoL products, they will be handled individually as units from a logistics perspective.

As pointed out in Section 3.3, we consider a disassembling of deep-discharged EVBS that workers with lower qualifications can disassemble than those who are not deep discharged. Accordingly, the wages for disassembly would be higher for second-life disassembly. The deep-discharging activity would be replaced by testing activities resulting in other fixed costs for equipment and a corresponding plant area for second-life purposes. Furthermore, additional requirements might increase costs for the construction of a plant.

Our used disassembling durations are retrieved from upscaling the battery. We have shown exemplarily in Section 4.2 that the disassembling duration can be decreased with deconstructive disassembly. However, we used the originally designed scenarios for the upscaling procedure. The upscaling was conducted based on expert knowledge and available online videos about disassembling different EVBSs. Unfortunately, the videos do not contain information about the actual (measured) disassembly duration. Analyzing the videos allows us to draw the conclusion that a standard procedure for the general sequence of disassembling steps exists. We only conducted a disassembling experiment with one battery system; more data about disassembling times and steps are needed to validate our disassembling time scaling. Nevertheless, as already discussed in Section 5.2, the resulting disassembling durations of our upscaling are in line with information given by the industry.

All in all, cost data must be fitted to individual use cases and depend on many factors. The results presented here should always be checked for transferability to other purposes. Disassembling costs have barely been addressed in EoL economic assessments of EVBSs, but they are essential for creating a circular traction battery supply chain.

Given that the number of BEV registrations is growing in Germany, the modeled return flows do not represent today's returns but will be reached in the future once higher amounts are returned. The EoL flows will incline exponentially as the new BEV registrations increase. It is highly interesting to plan an optimal network structure involving disassembly, collection, and recycling or repurposing costs from an economic perspective.

5.4. View on EVBS Disassembly Automation

The automation of EVBS disassembly is a highly discussed topic, and we have touched on it at some points within this paper. Consequently, we will shortly discuss how our results can be used in the context of EVBS disassembly automation.

Our results, especially from the video analysis, show that some common disassembling steps exist among all battery systems. This includes starting with the cover removal and retrieving the battery modules after removing busbars and other connections. However, the positioning of the modules and necessary components, such as the BMC, are different among the systems. Therefore, an automated disassembly system must follow a similar process but be adaptive for diverse battery systems.

Automated solutions for disassembly might not have to deal with all kinds of battery systems in some situations. If, for instance, vehicle producers set up their own reverse supply chain, the variety of battery systems that have to be dealt with decreases while the available information about the EoL EVBS increases. Thus, developing automation solutions can become more manageable, and it is also more likely that design for disassembly might be thought of more carefully during development.

As mentioned previously, our data from the disassembly experiment can help during the development of automation applications. A couple of principles can be formulated that, if followed during the battery system design phase, can help to (automate) disassembly activities. The list should not be understood as a complete list, and undoubtedly, not all principles can always be included in the design as many other factors than disassembly have to be considered during the design of a battery system.

- If screws are used, minimize the number of different screw heads to lower the number of needed tool changes.
- Use screws and plug connections instead of adhesives whenever possible or give instructions to best solve adhesive connections (examples: solvent, ultrasound)

- If non-destructive disassembly is the goal, minimize the number of different snap-fit connections.
- Screws should be accessible from a vertical position wherever possible or at least from the same direction for as many screws as possible.
- Supply accessible fixing points to secure the battery system during disassembly.
- Use modular construction that allows disassembly into sub-assemblies.
- Try to minimize the use of different materials in sub-assemblies, which is beneficial for further treatment and separation.
- Have connectors directly accessible whenever possible without having to remove other components.
- Have a fixed cable routing so that a robot will be less likely to get stuck during operation.
- Label the battery system with a unique code to retrieve disassembly instructions (example: QR code).

A potential solution to lower the needed task variety for the automation can be partial automation or a human–robotic collaboration in a more advanced setting [85]. In both settings, the robot performs the steps that contain high safety risks or need a lot of force, such as opening the cover. Automated solutions may be able to apply disassembly techniques that human workers cannot apply. The cover, for instance, may be opened by laser cutting [6]. Safety risks during disassembly may occur either through toxic substances or a high-voltage environment when the disassembly takes place for second-life usages of modules.

This paper's conducted time and cost estimation can serve as a benchmark for automation solutions. Automation will lead to a shift from variable labor costs to higher fixed costs, as fewer workers are involved. However, from today's perspective, it is not possible to determine how large an automated plant would have to be to achieve comparable costs. For such a calculation, the automation solutions still need further development. However, it is evident that in high labor cost countries, such as Germany or other central European countries, an automated disassembly solution will become economically profitable more quickly than in countries with lower labor costs.

6. Conclusions and Outlook

The disassembly of EVBSs will have increasing importance as the number of EoL traction batteries grows in the future. We conducted a disassembly experiment of a PHEV that allowed us to gain information about the disassembly process, needed tools, and the battery set-up.

Our analysis focused on the disassembly duration and how the different disassembly steps contribute to the overall disassembly time. We were able to address the measurement of uncertainty in disassembly duration by applying a fuzzy scheduling approach. The calculated disassembly durations were used to perform a cost estimation for a disassembly plant in Germany. The total disassembling costs per EVBS consist of fixed and variable costs and range from about 100 EUR/EVBS for small plants that decrease to 80 EUR/EVBS for large plants.

In our discussion section, we addressed each part of the results separately and discussed the most critical factors, which involve limits of the applied methods and their interpretation in a broader context, which is especially important for the cost and time calculations.

As the disassembling of electric vehicle systems is a young research field, many open questions remain and need to be addressed in the future. Examples are the automation potential of disassembling tasks or establishing reverse logistic networks. Furthermore, the reassembling for repurposing or refurbishing needs to be addressed and should be addressed together with disassembly.

Lastly, it should be noted that a shift to electric vehicle mobility will not only lead to an increasing number of EoL battery systems. Other obsolete EV components, such as electric motors, need disassembly actions. Thus, a circular EV supply chain goes beyond a circular battery supply chain.

Supplementary Materials: The following documents are available online at <https://www.mdpi.com/article/10.3390/en15155324/s1>, Supplementary Material S1: Detailed experiment's results (data and graphs), Supplementary Material S2: Explanation Cost Calculation; Supplementary Material S3: Table and graphs of video analysis [64,86–91].

Author Contributions: Conceptualization, S.R., S.B. and S.H.; methodology, S.R., S.H. and F.S.; validation, S.B.; formal analysis, S.R.; investigation, S.B., S.R., S.H. and A.A.A.; data curation, S.H.; writing—original draft preparation, S.R. and S.H.; writing—review and editing, S.B., S.G.-C. and F.S.; visualization, S.H. and S.R.; supervision, S.G.-C.; project administration, S.G.-C.; funding acquisition, S.G.-C. and F.S. All authors have read and agreed to the published version of the manuscript.

Funding: This research was funded by the Ministry of the Environment, Climate Protection and the Energy Sector Baden-Wuerttemberg for funding this work under the funding codes L7520104 and L7520101 as part of the accompanying research of the project “DeMoBat”.

Data Availability Statement: The data presented in this study are available within the article and the corresponding corresponding supplementary.

Acknowledgments: This manuscript is a result of the accompanying research of the project “DeMoBat—Disassembly of EV batteries and drive trains” (L7520104 and L7520101) funded by the federal agency for the environment Baden Wuerttemberg, Germany. The financial support is gratefully acknowledged. Furthermore, we acknowledge the support by the KIT-Publication Fund of the Karlsruhe Institute of Technology.

Conflicts of Interest: The authors declare no conflict of interest.

Nomenclature and Abbreviations

Abbreviations

BEV

BMC

CPM

EoL

EV

EVB

EVBS

FTE

HV

PHEV

Symbol

α

$\tilde{A} = \{(x, \mu_{\tilde{A}}(x)) \mid x \in X\}$ with $\mu_{\tilde{A}} : X \rightarrow [0, 1]$

$\tilde{A}_\alpha = \{x \in X \mid \mu_{\tilde{A}}(x) \geq \alpha\}$ with $\mu_{\tilde{A}} : X \rightarrow [0, 1]$

Bat^{new}

Bat^{org}

β

γ

$\tilde{D}_j = ({}_o d_j^\varepsilon, {}_o d_j^\lambda, {}_o d_j^1, {}_p d_j^1, {}_p d_j^\lambda, {}_p d_j^\varepsilon)$

\tilde{D}_j^{new}

\tilde{D}_j^{org}

ε

\tilde{EF}_j

\tilde{ES}_j

$F(\tilde{LF}_j)$

$hgt(\tilde{A}) = \sup_{x \in X} \mu_{\tilde{A}}(x)$

Translation

Battery electric vehicle

Battery management controller

Critical path method

End-of-Life

Electric vehicle

Electric vehicle battery

Electric vehicle battery system

Fulltime employee

High voltage

Plug-in hybrid vehicle

Meaning

Several membership levels

Fuzzy set \tilde{A}

α -level cuts of Interval \tilde{A}_α

Scaled battery module weight

Original battery module weight

Exponential scaling factor

Term for an additional disassembling time change

Fuzzy disassembling duration of activity j (six-point representation)

Scaled disassembly duration

Original disassembly duration

Membership level

Fuzzy earliest finish of activity j

Fuzzy earliest start of activity j

Defuzzified latest finish time step j

Height of normalized fuzzy set \tilde{A}

Symbol	Meaning
λ	Membership level
\widetilde{LF}_j	Fuzzy latest finish time of activity j
$\mu_{\widetilde{A}}$	Membership function $\in [0, 1]$
$\mu_{\widetilde{D}_j}(d_j)$	Membership function
\widetilde{T}	Latest completion time of the project
\widetilde{f}_j	Fuzzy finish time
\widetilde{s}_j	Fuzzy start time
\ominus	Subtraction
\oplus	Addition
\oplus^{inv}	Inverse addition

Appendix A

For a basic understanding of fuzzy logic and the underlying assumptions and mathematical operations, we direct the interested reader to [92,93].

The concept of fuzzy logic dates back to [37] and is founded on the fuzzy set theory. In fuzzy set theory, a multi-value membership function is used to indicate the membership of an object to a class, which is in contrast to the common binary membership of True or False [94]. This multi-value membership function allows presenting vagueness about the degree of membership of an object to a class.

Equation (A1) defines a fuzzy set \widetilde{A} [95]. The membership function $\mu_{\widetilde{A}}$ may take values in the interval of $[0, 1]$ and determines to which extent an element $x \in X$ belongs to the fuzzy set \widetilde{A} [26].

$$\widetilde{A} = \{(x, \mu_{\widetilde{A}}(x)) \mid x \in X\} \text{ with } \mu_{\widetilde{A}} : X \rightarrow [0, 1] \quad (\text{A1})$$

A fuzzy set \widetilde{A} is normalized by setting its height which is the supremum of the realized membership values, to 1 (Equation (A2)) [26].

$$\text{hgt}(\widetilde{A}) = \sup_{x \in X} \mu_{\widetilde{A}}(x) \quad (\text{A2})$$

To determine membership functions for use cases, experts can express information about optimistic and pessimistic values at one or several membership levels α . This is known as α -level cuts of a fuzzy interval \widetilde{A}_α and is defined in Equation (A3) [95]. A fuzzy interval contains one or more $x \in \mathbb{R}$ in a way that $\mu_{\widetilde{A}} = 1$ piecewise continues [34]. A fuzzy number contains only one $x \in \mathbb{R}$ with $\mu_{\widetilde{A}} = 1$ and is piecewise continues [34].

$$\widetilde{A}_\alpha = \{x \in X \mid \mu_{\widetilde{A}}(x) \geq \alpha\} \text{ with } \mu_{\widetilde{A}} : X \rightarrow [0, 1] \quad (\text{A3})$$

The use of fuzzy logic in this article is to calculate fuzzy disassembling durations. Each disassembling duration of an individual disassembling activity is expected to be a fuzzy number and can be used for calculation according to the proposed rules in Table 2. Nevertheless, it is important to mention that different authors propose different ways to use fuzzy numbers for arithmetic operations [96].

The application field of fuzzy logic is undoubtedly diverse. This can be shown, for instance, by looking at different research questions that have been addressed for electric vehicle battery systems. The authors of [97] have used fuzzy logic to set up a fuzzy logic-based adaptive control scheme for hybrid electric vehicles. The authors of [98] apply a fuzzy controller to improve the battery usage time. These are two examples of fuzzy logic within a technical engineering field of battery systems. Meanwhile, the authors of [99] apply fuzzy logic within a multi-criteria decision-making framework to select EoL recovery center locations. Nevertheless, both papers have in common that the fuzzy logic helps to model uncertain behavior that follows rules that can be described with linguistic variables.

Appendix B

Figure A1 shows the coordinates of the connections and the center of gravity of the parts. Here, the centers of gravity have been adjusted with an offset if the center of gravity is not located on the part surface. These points can be seen as gripping positions in automated disassembly solutions. The coordinates' numbers illustrated in Figure A1 can be found in the Supplementary Material S1.

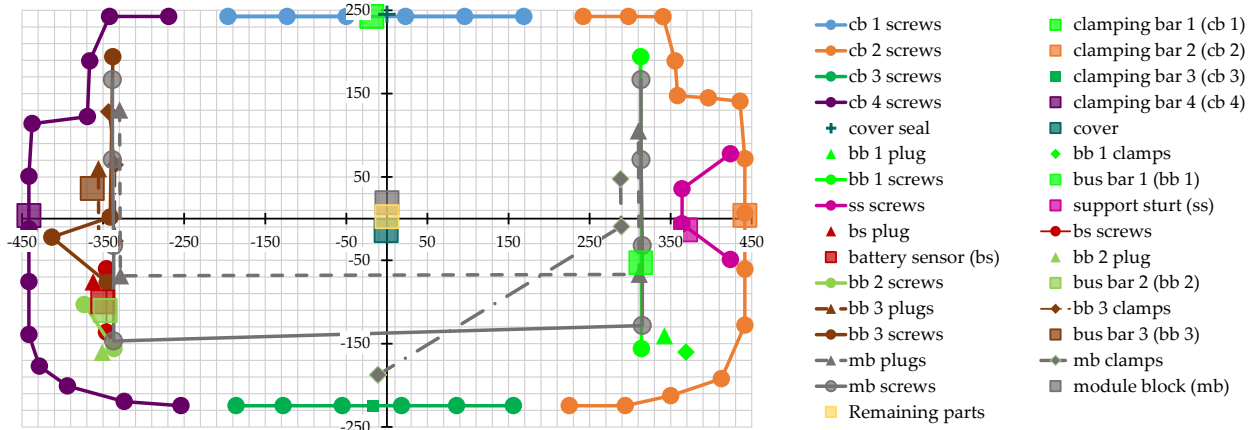


Figure A1. Disassembled battery system: XY-positions of the components and their connections; cb: clamping bars, mb: module block, bb: bus bar; bs: battery sensor.

Appendix C

Table A1. Description of fuzzy durations on a single activity basis.

Step <i>j</i>	Description of Included Activities
1	1.1 Screws are removed: $(3, 3.5, 4, 5, 5.5, 6) \times 40$ 1.2 Cutting of adhesive is time-consuming and less standardized (variation in duration expected): $(220, 300, 320, 380, 420, 450)$ 1.3 Remove of clamping bar by hand: $(1, 1.5, 2, 2, 2.5, 3) \times 4$ 1.4 Lift off upper cover and if necessary recut: $(5, 15, 20, 25, 30, 35)$
2	2.1 Screws identical to upper cover screw, removed with extension, add one second for extension: $(4, 4.5, 5, 6, 6.5, 6, 7) \times 2$ 2.2 Remove plugs with a combination of hand and hand screwdriver, variances may occur: $(8, 13, 15, 20, 22, 30) \times 2$ 2.3 Remove busbar by hand: $(1, 1.5, 2, 2, 2.5, 3)$
3	3.1 Screws are removed: $(3, 3.5, 4, 5, 5.5, 6) \times 4$ 3.2 Remove support strut by hand: $(1, 1.5, 2, 2, 2.5, 3)$
4	4.1 Remove air dryer; snap-on fasteners with latches are difficult to open because pressure points are poorly accessible; therefore, variance is expected: $(10, 12, 15, 20, 23, 25)$ 4.2 Open air dryer; force is needed, or experience; the variance is expected; own disassembling time was longer than expected in most cases: $(15, 20, 23, 27, 30, 35)$ 4.3 Remove plugs from BMC; variance expected; although different plugs, same time per plug in the calculation: $(4, 6, 7, 8, 9, 14) \times 6$ 4.4 Remove screw from interference suppression filter: $(3, 3.5, 4, 5, 5.5, 6)$ 4.5 Remove interference suppression filter by hand: $(1, 1.5, 2, 2, 2.5, 3)$ 4.6 Remove screws from air dryer bracket: $(3, 3.5, 4, 5, 5.5, 6) \times 2$ 4.7 Remove air dryer bracket by hand: $(1, 1.5, 2, 2, 2.5, 3)$ 4.8 Remove plug from interference suppression filter; pointed pliers is used (time for tool changing). Add 0.5 s per plug: $(4.5, 6.5, 7.5, 8.5, 9.5, 14.5) \times 5$ 4.9 Remove further plugs; poorly accessible; time comparable to 4.2: $(15, 20, 23, 27, 30, 35)$ 4.10 Remove screws from interference filter: $(3, 3.5, 4, 5, 5.5, 6) \times 3$ 4.11 Remove interference filter holder, took slightly longer than other removal by hand because of position (add 2 s): $(3, 3.5, 4, 4, 4.5, 5)$ 4.12 Remove screws from the BMC: $(3, 3.5, 4, 5, 5.5, 6) \times 2$ 4.13 Remove screws from the BMC; outside the battery cover, tool change; add 0.5 s per screw: $(3.5, 4, 4.5, 5.5, 6, 6.5) \times 4$ 4.14 Remove BMC by hand: $(1, 1.5, 2, 2, 2.5, 3)$ 4.15 Open BMC, comparable to snap-fastener of air dryer for removal, but two seconds faster: $(8, 10, 13, 18, 21, 23)$

Table A1. Cont.

Step <i>j</i>	Description of Included Activities
5	5.1 Remove screws from battery sensor with shunt: (3, 3.5, 4, 5, 5.5, 6) × 8
	5.2 Remove plug; better accessible than 4.8; 1.5 s less: (2.5, 4.5, 5.5, 6.5, 7.5, 12.5)
	5.3 Remove battery sensor with shunt by hand: (1, 1.5, 2, 2, 2.5, 3)
6	6.1 Remove screws from busbar 2: (3, 3.5, 4, 5, 5.5, 6) × 2
	6.2 Remove busbar 2 by hand: (1, 1.5, 2, 2, 2.5, 3)
	6.3 Remove power plugs and cable fixers; plugs and fixers are easily accessible and better accessible than 5.2; time equivalent to screws: (3, 3.5, 4, 5, 5.5, 6) × 5
	6.4 Remove screws from busbar 3 with integrated fuse: (3, 3.5, 4, 5, 5.5, 6) × 4
	6.5 Remove busbar 3 with integrated fuse: (1, 1.5, 2, 2, 2.5, 3)
	6.6 Remove screws on busbar 3; same time assumptions as for other screws, although they have slightly more weight: (3, 3.5, 4, 5, 5.5, 6) × 2
	6.7 Remove the fuse from busbar 3 by hand: (1, 1.5, 2, 2, 2.5, 3)
7	7.1 Remove plugs from console; comparable to 5.2: (2.5, 4.5, 5.5, 6.5, 7.5, 12.5) × 7
	7.2 Remove screws from console: (3, 3.5, 4, 5, 5.5, 6) × 5
	7.3 Remove console by hand: (1, 1.5, 2, 2, 2.5, 3)
	7.4 Remove plugs from wiring harness and relay; comparable to 7.1/5.2: (2.5, 4.5, 5.5, 6.5, 7.5, 12.5) × 2
	7.5 Remove screws and nut from series resistor; add 0.5 to screw time per screw to include change of tool to wrench: (3.5, 4, 4.5, 5.5, 6, 6.5) × 5
	7.6 Remove relay by hand: (1, 1.5, 2, 2, 2.5, 3)
	7.7 Remove screws from connectors: (3, 3.5, 4, 5, 5.5, 6) × 7
	7.8 Remove copper coils by hand: (1, 1.5, 2, 2, 2.5, 3) × 2
8	8.1 Remove screws from cables: (3, 3.5, 4, 5, 5.5, 6) × 2
	8.2 Remove plugs from filter; comparable to 5.2: (2.5, 4.5, 5.5, 6.5, 7.5, 12.5) × 2
	8.3 Remove screws between interference [. . .]; comparable to 5.2: (2.5, 4.5, 5.5, 6.5, 7.5, 12.5) × 2
	8.4 Remove screws between interference filter and battery cover: (3, 3.5, 4, 5, 5.5, 6) × 3
	8.5 Remove interference filter by hand: (1, 1.5, 2, 2, 2.5, 3)
	8.6 Remove screws to dismantle the interference filter: (3, 3.5, 4, 5, 5.5, 6) × 3
	8.7 Remove the top cover of the interference filter by hand: (1, 1.5, 2, 2, 2.5, 3)
9	9.1 Remove screws from HV connector form the outside of the cover: (3, 3.5, 4, 5, 5.5, 6) × 2
	9.2 Remove HV connector by hand: (1, 1.5, 2, 2, 2.5, 3)
	9.3 Remove screws inside console from orange component: (3, 3.5, 4, 5, 5.5, 6) × 2
	9.4 Remove orange component by hand: (1, 1.5, 2, 2, 2.5, 3)
	9.5 Open orange component to retrieve cover by hand: (1, 1.5, 2, 2, 2.5, 3)
	9.6 Remove diagnostic connector by hand: (1, 1.5, 2, 2, 2.5, 3)
10	10.1 Remove screws that connect modules to lower battery cover; screws are longer than others (add 0.5 s); change of bit set to keep the same tool (add 1 s): (4.5, 5, 5.5, 6.5, 6.5, 7.5) × 8
	10.2 Move lifting/pulling device (winch) to work station; assumed that it is provided closely without need to walk: (3, 3.5, 4, 5, 5.5, 6)
	10.3 Hook up the corner of the battery module to the lifting device and clamp the lower battery cover to the working station (screw clamps): (17, 20, 25, 30, 35, 37)
	10.4 Operate the winch by hand; Reference is a previously conducted experiment with a similar battery type: (17, 20, 25, 30, 35, 37)
	10.5 Place battery modules next to lower battery cover and unhook; release clamped lower batter cover): (17, 20, 25, 30, 35, 37)
	10.6 Put away lifting/pulling device: (3, 3.5, 4, 5, 5.5, 6)

Table A2. Fuzzy earliest start (\widetilde{ES}_j) of disassembly steps.

Step j	Calculation Fuzzy Earliest Start \widetilde{ES}_j	\widetilde{ES}_j [s]
0	t_0	(0, 0, 0, 0, 0, 0)
1	$\max \left\{ \widetilde{ES}_0 \oplus \widetilde{D}_0 \right\}$	(0, 0, 0, 0, 0, 0)
2	$\max \left\{ \widetilde{ES}_1 \oplus \widetilde{D}_1 \right\}$	(349, 461, 508, 615, 680, 737)
3	$\max \left\{ \widetilde{ES}_2 \oplus \widetilde{D}_2 \right\}$	(374, 497.5, 550, 667, 739.5, 814)
4	$\max \left\{ \widetilde{ES}_3 \oplus \widetilde{D}_3 \right\}$	(387, 513, 568, 689, 764, 841)
5	$\max \left\{ \widetilde{ES}_1 \oplus \widetilde{D}_1 \right\}$	(349, 461, 508, 615, 680, 737)
6	$\max \left\{ \widetilde{ES}_5 \oplus \widetilde{D}_5 \right\}$	(376.5, 495, 547.5, 661.5, 734, 800.5)
7	$\max \left\{ \widetilde{ES}_6 \oplus \widetilde{D}_6 \right\}$	(407.5, 532.5, 591.5, 714.5, 793.5, 866.5)
8	$\max \left\{ \widetilde{ES}_7 \oplus \widetilde{D}_7 \right\}$	(487.5, 641, 719.5, 868.5, 967, 1095.5)
9	$\max \left\{ \begin{matrix} \widetilde{ES}_0 \oplus \widetilde{D}_0, \\ \widetilde{ES}_8 \oplus \widetilde{D}_8 \end{matrix} \right\}$	(523.5, 690, 777.5, 938.5, 1046, 1199.5)
10	$\max \left\{ \begin{matrix} \widetilde{ES}_3 \oplus \widetilde{D}_3, \\ \widetilde{ES}_6 \oplus \widetilde{D}_6 \end{matrix} \right\}$	(407.5, 532.5, 591.5, 714.5, 793.5, 866.5)
11	$\max \left\{ \begin{matrix} \widetilde{ES}_4 \oplus \widetilde{D}_4, \\ \widetilde{ES}_9 \oplus \widetilde{D}_9, \\ \widetilde{ES}_{10} \oplus \widetilde{D}_{10} \end{matrix} \right\}$	(539.5, 710, 801.5, 966.5, 1078, 1235.5)

Table A3. Fuzzy latest finish times (\widetilde{LF}_j) of disassembling steps.

Step j	Calculation Fuzzy Latest Finish \widetilde{LF}_j	\widetilde{LF}_j [s]
0	$\min \left\{ \begin{matrix} \widetilde{LF}_1 \oplus^{inv} \widetilde{D}_1, \\ \widetilde{LF}_9 \oplus^{inv} \widetilde{D}_9 \end{matrix} \right\}$	(0, 0, 0, 0, 0, 0)
1	$\min \left\{ \begin{matrix} \widetilde{LF}_2 \oplus^{inv} \widetilde{D}_2, \\ \widetilde{LF}_5 \oplus^{inv} \widetilde{D}_5 \end{matrix} \right\}$	(349, 461, 508, 615, 680, 737)
2	$\min \left\{ \widetilde{LF}_3 \oplus^{inv} \widetilde{D}_3 \right\}$	(388, 512, 570, 690, 768, 846)
3	$\min \left\{ \begin{matrix} \widetilde{LF}_4 \oplus^{inv} \widetilde{D}_4, \\ \widetilde{LF}_{10} \oplus^{inv} \widetilde{D}_{10} \end{matrix} \right\}$	(401, 527.5, 588, 712, 792.5, 873)
4	$\min \left\{ \widetilde{LF}_{11} \oplus^{inv} \widetilde{D}_{11} \right\}$	(487.5, 641, 719.5, 868.5, 967, 1095.5)
5	$\min \left\{ \widetilde{LF}_6 \oplus^{inv} \widetilde{D}_6 \right\}$	(376.5, 495, 547.5, 661.5, 734, 800.5)
6	$\min \left\{ \begin{matrix} \widetilde{LF}_7 \oplus^{inv} \widetilde{D}_7, \\ \widetilde{LF}_{10} \oplus^{inv} \widetilde{D}_{10} \end{matrix} \right\}$	(407.5, 532.5, 591.5, 714.5, 793.5, 866.5)
7	$\min \left\{ \widetilde{LF}_8 \oplus^{inv} \widetilde{D}_8 \right\}$	(487.5, 641, 719.5, 868.5, 967, 1095.5)
8	$\min \left\{ \widetilde{LF}_9 \oplus^{inv} \widetilde{D}_9 \right\}$	(523.5, 690, 777.5, 935.5, 1046, 1199.5)
9	$\min \left\{ \widetilde{LF}_{11} \oplus^{inv} \widetilde{D}_{11} \right\}$	(539.5, 710, 801.5, 966.5, 1078, 1235.5)
10	$\min \left\{ \widetilde{LF}_{11} \oplus^{inv} \widetilde{D}_{11} \right\}$	(539.5, 710, 801.5, 966.5, 1078, 1235.5)
11	$\widetilde{T} = \widetilde{EF}_{11} - \widetilde{ES}_9$	(539.5, 710, 801.5, 966.5, 1078, 1235.5)

Table A4. Scenario “One worker” resulting fuzzy start time (\tilde{t}_j^s) and fuzzy finish time (\tilde{t}_j^f).

Planning Order	Step j	Fuzzy Start Time [s] $\tilde{t}_j^s = (o t_j^{s^{0.1}}, o t_j^{s^{0.6}}, o t_j^{s^1}, p t_j^{s^1}, p t_j^{s^{0.6}}, p t_j^{s^{0.1}})$	Fuzzy Finish Time [s] $\tilde{t}_j^f = (o t_j^{f^{0.1}}, o t_j^{f^{0.6}}, o t_j^{f^1}, p t_j^{f^1}, p t_j^{f^{0.6}}, p t_j^{f^{0.1}})$
1	0	(0, 0, 0, 0, 0, 0)	(0, 0, 0, 0, 0, 0)
2	1	(0, 0, 0, 0, 0, 0)	(349, 461, 508, 615, 680, 737)
3	5	(349, 461, 508, 615, 680, 737)	(376.5, 495, 547.5, 661.5, 734, 800.5)
4	2	(376.5, 495, 547.5, 661.5, 734, 800.5)	(401.5, 531.5, 589.5, 715.5, 793.5, 877.5)
5	3	(401.5, 531.5, 589.5, 715.5, 793.5, 877.5)	(414.5, 547, 607.5, 735.5, 818, 904.5)
6	6	(414.5, 547, 607.5, 735.5, 818, 904.5)	(445.5, 584.5, 651.5, 790.5, 877.5, 970.5)
7	7	(445.5, 584.5, 651.5, 790.5, 877.5, 970.5)	(525.5, 693, 779.5, 944.5, 1051, 1199.5)
8	8	(525.5, 693, 779.5, 944.5, 1051, 1199.5)	(561.5, 742, 837.5, 1014.5, 1130, 1303.5)
9	4	(561.5, 742, 837.5, 1014.5, 1130, 1303.5)	(700, 924.5, 1051, 1269, 1415.5, 1666)
10	9	(700, 924.5, 1051, 1269, 1415.5, 1666)	(716, 944.5, 1075, 1297, 1447.5, 1702)
11	10	(716, 944.5, 1075, 1297, 1447.5, 1702)	(809, 1051.5, 1202, 1449, 1589.5, 1888)
12	11	(809, 1051.5, 1202, 1449, 1589.5, 1888)	(809, 1051.5, 1202, 1449, 1589.5, 1888)

Table A5. Scenario “Two workers” resulting fuzzy start time (\tilde{t}_j^s) and fuzzy finish time (\tilde{t}_j^f).

Planning Order	Worker One Step j	Worker Two Step j	Fuzzy Start Time [s] $\tilde{t}_j^s = (o t_j^{s^{0.1}}, o t_j^{s^{0.6}}, o t_j^{s^1}, p t_j^{s^1}, p t_j^{s^{0.6}}, p t_j^{s^{0.1}})$	Fuzzy Finish Time [s] $\tilde{t}_j^f = (o t_j^{f^{0.1}}, o t_j^{f^{0.6}}, o t_j^{f^1}, p t_j^{f^1}, p t_j^{f^{0.6}}, p t_j^{f^{0.1}})$
1			(0, 0, 0, 0, 0, 0)	(0, 0, 0, 0, 0, 0)
2	1		(0, 0, 0, 0, 0, 0)	(349, 461, 508, 615, 680, 737)
3	5		(349, 461, 508, 615, 680, 737)	(376.5, 495, 547.5, 661.5, 734, 800.5)
3		2	(349, 461, 508, 615, 680, 737)	(374, 497.5, 550, 667, 739.5, 814)
4	6		(376.5, 495, 547.5, 661.5, 734, 800.5)	(407.5, 532.5, 591.5, 714.5, 793.5, 866.5)
5		3	(374, 497.5, 550, 667, 739.5, 814)	(387, 513, 568, 689, 764, 841)
6		4	(387, 513, 568, 689, 764, 841)	(525.5, 695.5, 781.5, 943.5, 1049.5, 1203.5)
7	7		(407.5, 532.5, 591.5, 714.5, 793.5, 866.5)	(487.5, 641, 719.5, 868.5, 967, 1095.5)
8	8		(487.5, 641, 719.5, 868.5, 967, 1095.5)	(523.5, 690, 777.5, 938.5, 1046, 1199.5)
9	9		(523.5, 690, 777.5, 938.5, 1046, 1199.5)	(539.5, 710, 801.5, 966.5, 1078, 1235.5)
10		10	(525.5, 695.5, 781.5, 943.5, 1049.5, 1203.5)	(618, 802.5, 908.5, 1095.5, 1191.5, 1389.5)
11			(618, 802.5, 908.5, 1095.5, 1191.5, 1389.5)	(618, 802.5, 908.5, 1095.5, 1191.5, 1389.5)

Table A6. Scenario “Two workers, cover together” resulting fuzzy start time (\tilde{t}_j^s) and fuzzy finish time (\tilde{t}_j^f).

Planning Order	Worker One Step j	Worker Two Step j	Fuzzy Start Time [s] $\tilde{t}_j^s = (o t_j^{s^{0.1}}, o t_j^{s^{0.6}}, o t_j^{s^1}, p t_j^{s^1}, p t_j^{s^{0.6}}, p t_j^{s^{0.1}})$	Fuzzy Finish Time [s] $\tilde{t}_j^f = (o t_j^{f^{0.1}}, o t_j^{f^{0.6}}, o t_j^{f^1}, p t_j^{f^1}, p t_j^{f^{0.6}}, p t_j^{f^{0.1}})$
1			(0, 0, 0, 0, 0, 0)	(0, 0, 0, 0, 0, 0)
2	1	1	(0, 0, 0, 0, 0, 0)	(174.5, 230.50, 254, 306.5, 340, 368.5)
3	2		(174.5, 230.50, 254, 306.5, 340, 368.5)	(199.5, 267, 296, 306.5, 399.5, 445.5)
3		5	(174.5, 230.50, 254, 306.5, 340, 368.5)	(202, 264.5, 293.5, 355, 394, 432)
4		6	(202, 264.5, 293.5, 355, 394, 432)	(232, 302, 337.5, 408, 453.5, 498)
5	3		(199.5, 267, 296, 306.5, 399.5, 445.5)	(212.5, 282.5, 314, 382.5, 424, 472.5)
6	4		(212.5, 282.5, 314, 382.5, 424, 472.5)	(351, 465, 527.5, 637, 709.5, 835)
7		7	(232, 302, 337.5, 408, 453.5, 498)	(313, 410.5, 465.5, 562.5, 627, 727)
8		8	(313, 410.5, 465.5, 562.5, 627, 727)	(349, 459.5, 523.5, 632, 706, 831)
9		9	(349, 459.5, 523.5, 632, 706, 831)	(365, 479.5, 547.5, 660, 738, 867)
10	10		(351, 465, 527.5, 637, 709.5, 835)	(444, 572, 654.5, 789, 851.5, 1021)
11			(444, 572, 654.5, 789, 851.5, 1021)	(444, 572, 654.5, 789, 851.5, 1021)

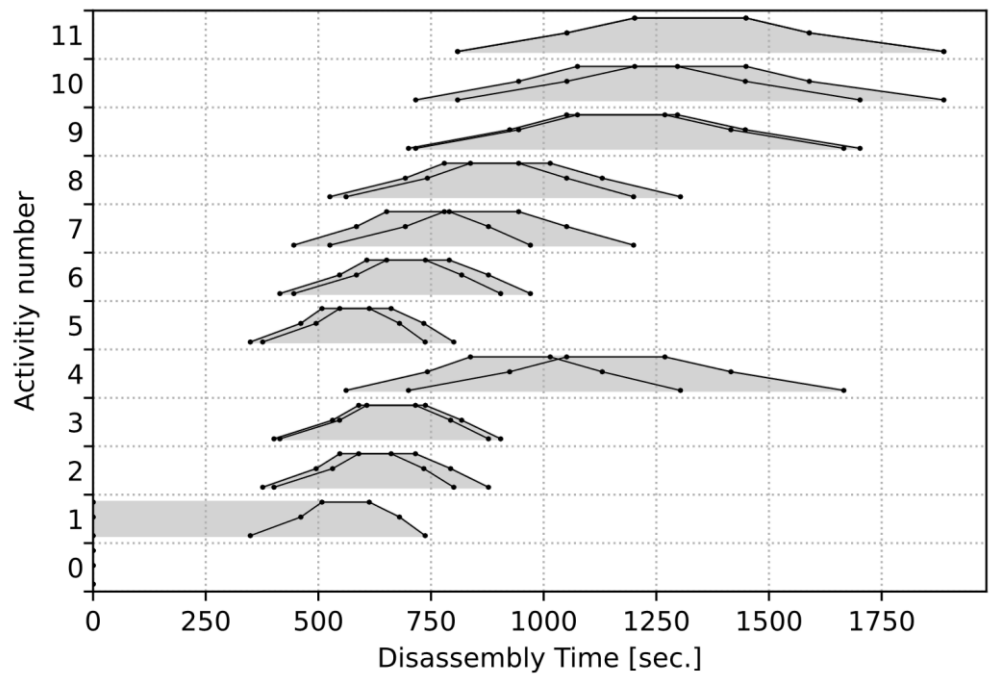


Figure A2. Scenario “One worker” resulting fuzzy Gantt chart for each disassembling step and calculated their fuzzy start time (\tilde{t}_j^s) and fuzzy finish time (\tilde{t}_j^f).

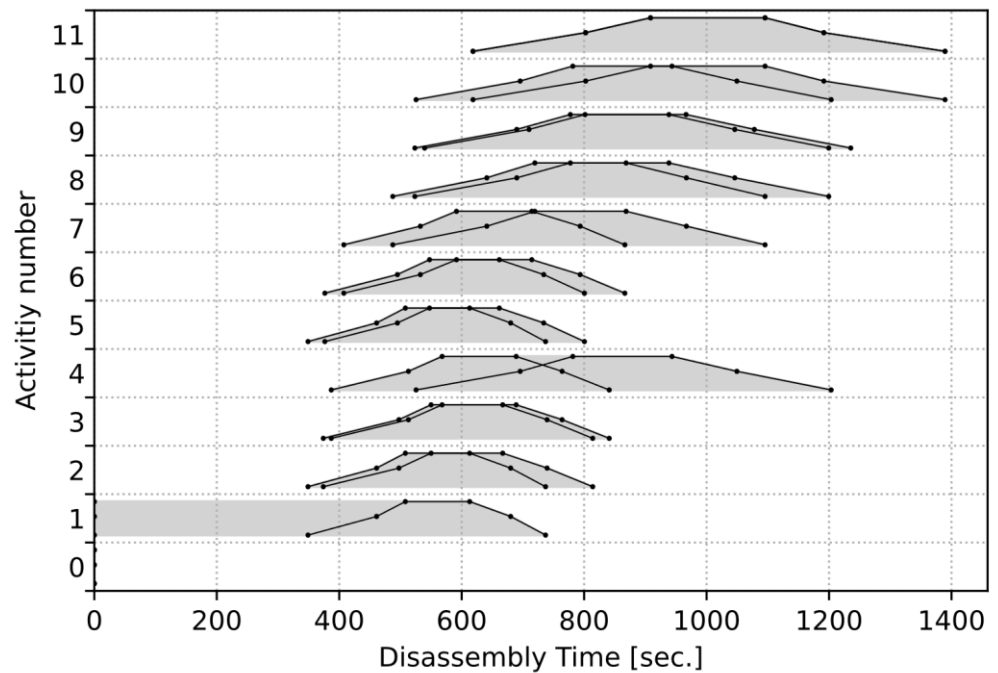


Figure A3. Scenario “Two Workers”: resulting fuzzy Gantt chart for each disassembling step.

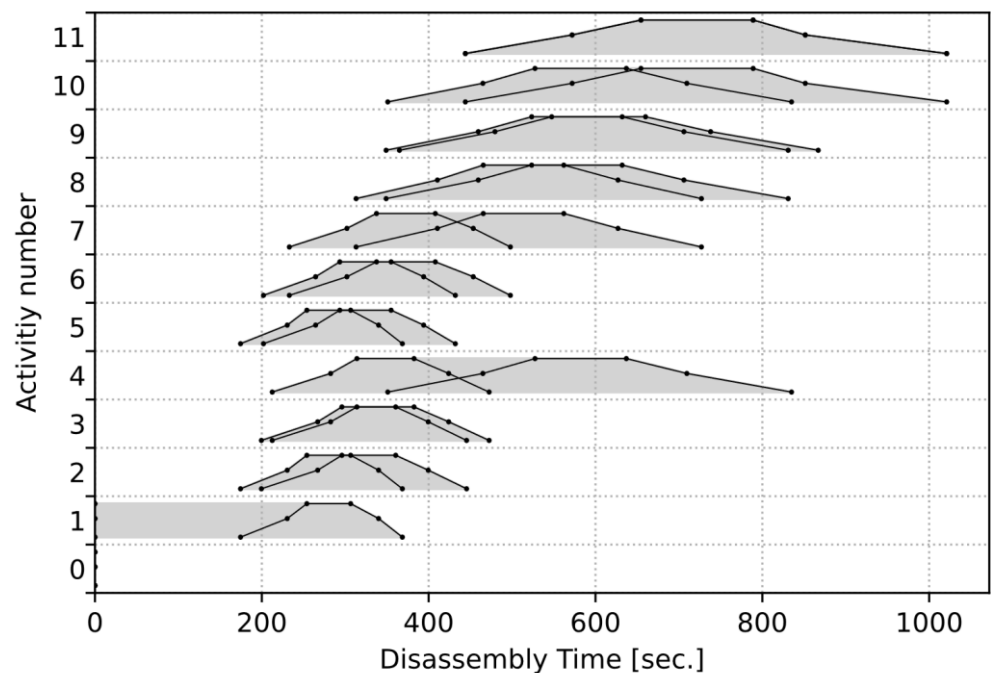


Figure A4. Scenario “Two Workers, cover together”: resulting fuzzy Gantt chart for each disassembling step and calculated fuzzy start time (\tilde{t}_j^s) and fuzzy finish time (\tilde{t}_j^f).

References

1. European Commission. The European Green Deal (COM(2019) 640 Final). 2019. Available online: <https://eur-lex.europa.eu/legal-content/EN/TXT/?uri=CELEX%3A52019DC0640&qid=1639045060648> (accessed on 8 December 2021).
2. European Commission. A Clean Planet for all: A European Strategic Long-Term Vision for a Prosperous, Modern, Competitive and Climate Neutral Economy (COM(2018) 773 Final). 2018. Available online: <https://eur-lex.europa.eu/legal-content/EN/ALL/?uri=COM%3A2018%3A773%3AFIN> (accessed on 8 December 2021).
3. European Commission. A New Circular Economy Action Plan for a Cleaner and More Competitive Europe (COM(2020) 98 Final). 2020. Available online: <https://eur-lex.europa.eu/legal-content/EN/TXT/?qid=1583933814386&uri=COM:2020:98:FIN> (accessed on 8 December 2021).
4. Pagliaro, M.; Meneguzzo, F. Lithium battery reusing and recycling: A circular economy insight. *Heliyon* **2019**, *5*, e01866. [CrossRef] [PubMed]
5. Glöser-Chahoud, S.; Huster, S.; Rosenberg, S.; Baazouzi, S.; Kiemel, S.; Singh, S.; Schneider, C.; Weeber, M.; Mieke, R.; Schultmann, F. Industrial disassembling as a key enabler of circular economy solutions for obsolete electric vehicle battery systems. *Resour. Conserv. Recycl.* **2021**, *174*, 105735. [CrossRef]
6. Baazouzi, S.; Rist, F.P.; Weeber, M.; Birke, K.P. Optimization of disassembly strategies for electric vehicle batteries. *Batteries* **2021**, *7*, 74. [CrossRef]
7. Baars, J.; Domenech, T.; Bleischwitz, R.; Melin, H.E.; Heidrich, O. Circular economy strategies for electric vehicle batteries reduce reliance on raw materials. *Nat. Sustain.* **2021**, *4*, 71–79. [CrossRef]
8. Moore, E.A.; Russell, J.D.; Babbitt, C.W.; Tomaszewski, B.; Clark, S.S. Spatial modeling of a second-use strategy for electric vehicle batteries to improve disaster resilience and circular economy. *Resour. Conserv. Recycl.* **2020**, *160*, 104889. [CrossRef]
9. Kirchherr, J.; Reike, D.; Hekkert, M. Conceptualizing the circular economy: An analysis of 114 definitions. *Resour. Conserv. Recycl.* **2017**, *127*, 221–232. [CrossRef]
10. Alfaro-Algaba, M.; Ramirez, F.J. Techno-economic and environmental disassembly planning of lithium-ion electric vehicle battery packs for remanufacturing. *Resour. Conserv. Recycl.* **2020**, *154*, 104461. [CrossRef]
11. Windisch-Kern, S.; Gerold, E.; Nigl, T.; Jandric, A.; Altendorfer, M.; Rutrecht, B.; Scherhauser, S.; Raupenstrauch, H.; Pomberger, R.; Antrekowitsch, H.; et al. Recycling chains for lithium-ion batteries: A critical examination of current challenges, opportunities and process dependencies. *Waste Manag.* **2022**, *138*, 125–139. [CrossRef]
12. Li, L.; Zheng, P.; Yang, T.; Sturges, R.; Ellis, M.W.; Li, Z. Disassembly automation for recycling end-of-life lithium-ion pouch cells. *JOM* **2019**, *71*, 4457–4464. [CrossRef]
13. Marshall, J.; Gastol, D.; Sommerville, R.; Middleton, B.; Goodship, V.; Kendrick, E. Disassembly of Li ion cells—characterization and safety considerations of a recycling scheme. *Metals* **2020**, *10*, 773. [CrossRef]
14. Elwert, T.; Goldmann, D.; Römer, F.; Buchert, M.; Merz, C.; Schueler, D.; Sutter, J. Current developments and challenges in the recycling of key components of (hybrid) electric vehicles. *Recycling* **2016**, *1*, 25–60. [CrossRef]

15. Lisbona, D.; Snee, T. A review of hazards associated with primary lithium and lithium-ion batteries. *Process Saf. Environ. Prot.* **2011**, *89*, 434–442. [[CrossRef](#)]
16. Gumanova, V.; Sobotova, L. Proposal for disassembly of electric vehicle batteries used in the volkswagen jetta hybrid system. In Proceedings of the 2019 International Council on Technologies of Environmental Protection (ICTEP), Stary Smokovec, Slovakia, 23–25 October 2019; pp. 100–106.
17. Wegener, K.; Andrew, S.; Raatz, A.; Dröder, K.; Herrmann, C. Disassembly of electric vehicle batteries using the example of the audi Q5 hybrid system. *Procedia CIRP* **2014**, *23*, 155–160. [[CrossRef](#)]
18. Rallo, H.; Benveniste, G.; Gestoso, I.; Amante, B. Economic analysis of the disassembling activities to the reuse of electric vehicles Li-ion batteries. *Resour. Conserv. Recycl.* **2020**, *159*, 104785. [[CrossRef](#)]
19. Hellmuth, J.F.; DiFilippo, N.M.; Jouaneh, M.K. Assessment of the automation potential of electric vehicle battery disassembly. *J. Manuf. Syst.* **2021**, *59*, 398–412. [[CrossRef](#)]
20. Gerlitz, E.; Greifenstein, M.; Hofmann, J.; Fleischer, J. Analysis of the variety of lithium-ion battery modules and the challenges for an agile automated disassembly system. *Procedia CIRP* **2021**, *96*, 175–180. [[CrossRef](#)]
21. Herrmann, C.; Raatz, A.; Mennenga, M.; Schmitt, J.; Andrew, S. Assessment of automation potentials for the disassembly of automotive lithium ion battery systems. In *Leveraging Technology for a Sustainable World*; Dornfeld, D.A., Linke, B.S., Eds.; Springer: Berlin/Heidelberg, Germany, 2012; pp. 149–154.
22. Wegener, K.; Chen, W.H.; Dietrich, F.; Dröder, K.; Kara, S. Robot assisted disassembly for the recycling of electric vehicle batteries. *Procedia CIRP* **2015**, *29*, 716–721. [[CrossRef](#)]
23. Garrido-Hidalgo, C.; Ramirez, F.J.; Olivares, T.; Roda-Sanchez, L. The adoption of internet of things in a circular supply chain framework for the recovery of WEEE: The case of lithium-ion electric vehicle battery packs. *Waste Manag.* **2020**, *103*, 32–44. [[CrossRef](#)] [[PubMed](#)]
24. Tan, W.J.; Chin, C.M.M.; Garg, A.; Gao, L. A hybrid disassembly framework for disassembly of electric vehicle batteries. *Int. J. Energy Res.* **2021**, *45*, 8073–8082. [[CrossRef](#)]
25. Lander, L.; Cleaver, T.; Rajaeifar, M.A.; Nguyen-Tien, V.; Elliott, R.J.; Heidrich, O.; Kendrick, E.; Edge, J.S.; Offer, G. Financial viability of electric vehicle lithium-ion battery recycling. *Isience* **2021**, *24*, 102787. [[CrossRef](#)]
26. Schultmann, F. *Stoffstrombasiertes Produktionsmanagement: Betriebswirtschaftliche Planung und Steuerung Industrieller Kreislaufwirtschaftssysteme*; Erich Schmidt: Berlin, Germany, 2003; Volume 58.
27. Nguyen, H.T.; Walker, E.A.; Walker, E. *A First Course in Fuzzy Logic*, 2nd ed.; Chapman & Hall/CRC: Boca Raton, FL, USA, 2020.
28. Liang, J.; Guo, S.; Zhang, Y.; Liu, W.; Zhou, S. Energy-efficient optimization of two-sided disassembly line balance considering parallel operation and uncertain using multiobjective flatworm algorithm. *Sustainability* **2021**, *13*, 3358. [[CrossRef](#)]
29. Bentaha, M.L.; Battaia, O.; Dolgui, A.; Hu, S.J. Dealing with uncertainty in disassembly line design. *CIRP Ann.* **2014**, *63*, 21–24. [[CrossRef](#)]
30. Ke, Q.; Zhang, P.; Zhang, L.; Song, S. Electric vehicle battery disassembly sequence planning based on frame-subgroup structure combined with genetic algorithm. *Front. Mech. Eng.* **2020**, *6*, 576642. [[CrossRef](#)]
31. Shaocheng, T. Interval number and fuzzy number linear programmings. *Fuzzy Sets Syst.* **1994**, *66*, 301–306. [[CrossRef](#)]
32. Hapke, M.; Slowinski, R. Fuzzy priority heuristics for project scheduling. *Fuzzy Sets Syst.* **1996**, *83*, 291–299. [[CrossRef](#)]
33. Sadollah, A. *Fuzzy Logic Based in Optimization Methods and Control Systems and Its Applications*; InTechOpen: London, UK, 2018.
34. Rommelfanger, H. Fuzzy decision support-systeme: Entscheiden bei Unschärfe. In *Springer-Lehrbuch*, 2nd ed.; Springer: Berlin/Heidelberg, Germany, 1994.
35. Radot, A.D.; Rakshit, A. A ‘fuzzy’ approach to facilities lay-out planning. *Int. J. Prod. Res.* **1991**, *29*, 835–857. [[CrossRef](#)]
36. Schultmann, F.; Rentz, O. Fuzzy scheduling for the dismantling of complex products. In *Operations Research, Proceedings of the 2002: Selected Papers of the International Conference on Operations Research (SOR 2002)*, Klagenfurt, Austria, 2–5 September 2002; Leopold-Wildburger, U., Ed.; Springer: Berlin/Heidelberg, Germany, 2003; pp. 302–307.
37. Zadeh, L.A. Fuzzy sets. *Inf. Control.* **1965**, *8*, 338–353. [[CrossRef](#)]
38. Schultmann, F.; Fröhling, M.; Rentz, O. Fuzzy approach for production planning and detailed scheduling in paints manufacturing. *Int. J. Prod. Res.* **2006**, *44*, 1589–1612. [[CrossRef](#)]
39. Bhunia, A.K.; Sahoo, L.; Shaikh, A.A. Project management. In *Advanced Optimization and Operations Research*; Bhunia, A.K., Sahoo, L., Shaikh, A.A., Eds.; Springer: Singapore, 2019; Volume 153, pp. 367–402.
40. Hapke, M.; Jaskiewicz, A.; Słowiński, R. Fuzzy multi-mode resource-constrained project scheduling with multiple objectives. In *Project Scheduling*; Hillier, F.S., Węglarz, J., Eds.; Springer: Boston, MA, USA, 1999; Volume 14, pp. 353–380.
41. Wang, K. Computational intelligence in agile manufacturing engineering. In *Agile Manufacturing: The 21st Century Competitive Strategy*; Gunasekaran, A., Ed.; Elsevier: Amsterdam, The Netherlands, 2001; pp. 297–315.
42. Cho, J.-H.; Kim, Y.-D. A simulated annealing algorithm for resource constrained project scheduling problems. *J. Oper. Res. Soc.* **1997**, *48*, 736–744. [[CrossRef](#)]
43. Hapke, M.; Jaskiewicz, A.; Slowinski, R. Fuzzy project scheduling system for software development. *Fuzzy Sets Syst.* **1994**, *67*, 101–117. [[CrossRef](#)]
44. Hapke, M.; Słowiński, R. Fuzzy set approach to multi-objective and multi-mode project scheduling under uncertainty. In *Scheduling under fuzziness: With 29 Tables*; Słowiński, R., Ed.; Physica-Verlag: Heidelberg, Germany, 2000; pp. 197–221.

45. Kwade, A.; Bärwaldt, G. Recycling von Lithium-Ionen-Batterien im Rahmen des FuE-Programms. Förderung von Forschung und Entwicklung im Bereich der Elektromobilität. Abschlussbericht, Braunschweig, Germany. 2012. Available online: <https://www.erneuerbar-mobil.de/sites/default/files/publications/abschlussbericht-lithorec.pdf> (accessed on 26 November 2021).
46. Thies, C.; Kieckhäfer, K.; Hoyer, C.; Spengler, T.S. Economic assessment of the lithorec process. In *Recycling of Lithium-Ion Batteries: The LithoRec Way*; Kwade, A., Diekmann, J., Eds.; Springer: Cham, Switzerland, 2018.
47. Dai, Q.; Spangenberg, J.; Ahmed, S.; Gaines, L.; Kelly, J.C.; Wang, M. *EverBatt: A Closed-Loop Battery Recycling Cost and Environmental Impacts Model*; Argonne National Lab.(ANL): Argonne, IL, USA, 2019. [CrossRef]
48. Lambert, A.J.D.; Gupta, S.M. Disassembly modeling for assembly, maintenance, reuse, and recycling. In *The St. Lucie Press Series on Resource Management*; CRC Press: Boca Raton, FL, USA, 2005.
49. Vanegas Pena, P.; Peeters, J.; Cattrysse, D.; Duflou, J.; Tecchio, P.; Mathieux, F.; Ardente, F. *Study for a Method to Assess the Ease of Disassembly of Electrical and Electronic Equipment: Method Development and Application to a Flat Panel Display Case Study*; Publications Office of the European Union: Luxembourg, 2016.
50. Asiedu, Y.; Gu, P. Product life cycle cost analysis: State of the art review. *Int. J. Prod. Res.* **1998**, *36*, 883–908. [CrossRef]
51. Kroll, E. Application of work-measurement analysis to product disassembly for recycling. *Concurr. Eng.* **1996**, *4*, 149–158. [CrossRef]
52. Mandolini, M.; Favi, C.; Germani, M.; Marconi, M. Time-based disassembly method: How to assess the best disassembly sequence and time of target components in complex products. *Int. J. Adv. Manuf. Technol.* **2018**, *95*, 409–430. [CrossRef]
53. Desai, A.; Mital, A. Evaluation of disassemblability to enable design for disassembly in mass production. *Int. J. Ind. Ergon.* **2003**, *32*, 265–281. [CrossRef]
54. Vanegas, P.; Peeters, J.R.; Cattrysse, D.; Tecchio, P.; Ardente, F.; Mathieux, F.; Dewulf, W.; Duflou, J.R. Ease of disassembly of products to support circular economy strategies. *Resour. Conserv. Recycl.* **2018**, *135*, 323–334. [CrossRef] [PubMed]
55. Boks, C.B.; Kroll, E.; Brouwers, W.; Stevels, A. Disassembly modeling: Two applications to a Philips 21" television set. In Proceedings of the 1996 IEEE International Symposium on Electronics and the Environment. ISEE-1996, Dallas, TX, USA, 6–8 May 1996; pp. 224–229.
56. McGlothlin, S.; Kroll, E. Systematic estimation of disassembly difficulties: Application to computer monitors. In Proceedings of the 1995 IEEE International Symposium on Electronics and the Environment ISEE (Cat. No.95CH35718), Orlando, FL, USA, 1–3 May 1995; pp. 83–88.
57. Favi, C.; Marconi, M.; Germani, M.; Mandolini, M. A design for disassembly tool oriented to mechatronic product de-manufacturing and recycling. *Adv. Eng. Inform.* **2019**, *39*, 62–79. [CrossRef]
58. Kroll, E.; Carver, B.S. Disassembly analysis through time estimation and other metrics. *Robot. Comput. Integr. Manuf.* **1999**, *15*, 191–200. [CrossRef]
59. Das, S.K.; Yedlarajiah, P.; Narendra, R. An approach for estimating the end-of-life product disassembly effort and cost. *Int. J. Prod. Res.* **2000**, *38*, 657–673. [CrossRef]
60. Recchioni, M.; Ardente, F. *Environmental Footprint and Material Efficiency Support for Product Policy: Feasibility Study for a Standardised Method to Measure the Time Taken to Extract Certain Parts from Electrical and Electronic Equipment (JRC84311)*; Publications Office of the European Union: Luxembourg, 2016. Available online: <https://op.europa.eu/s/nxGV> (accessed on 15 May 2022).
61. Fulvio, A.; Fabrice, M.; Marco, R. Recycling of electronic displays: Analysis of pre-processing and potential ecodesign improvements. *Resour. Conserv. Recycl.* **2014**, *92*, 158–171. [CrossRef]
62. Salhofer, S.; Spitzbart, M.; Maurer, K. Recycling of LCD screens in europe-state of the art and challenges. In *Glocalized Solutions for Sustainability in Manufacturing, Proceedings of the 18th CIRP International Conference on Life Cycle Engineering, Technische Universität Braunschweig, Braunschweig, Germany, 2–4 May 2011*; Hesselbach, J., Ed.; Springer: Berlin/Heidelberg, Germany, 2011.
63. IEA. Global EV Outlook 2020: Entering the Decade of Electric Drive? 2020. Available online: <https://www.iea.org/reports/global-ev-outlook-2020#the-global-electric-vehicle-fleet-expanded-significantly-over-the-last-decade-underpinned-by-supportive-policies-and-technology-advances> (accessed on 9 May 2022).
64. Malmberg, C.J. Facility design: The block layout planning process for manufacturing systems. In *Handbook of Design, Manufacturing and Automation*; Dorf, R.C., Kusiak, A., Eds.; John Wiley & Sons, Inc.: Hoboken, NJ, USA, 1994; pp. 461–479.
65. Sawanishi, H.; Torihara, K.; Mishima, N. A study on disassemblability and feasibility of component reuse of mobile phones. *Procedia CIRP* **2015**, *26*, 740–745. [CrossRef]
66. Stevels, A. Applied EcoDesign Take Back & Recycling. Available online: <https://slidetodoc.com/applied-eco-design-take-back-recycling-prof-dr/> (accessed on 2 May 2022).
67. Sodhi, R.; Sonnenberg, M.; Das, S. Evaluating the unfastening effort in design for disassembly and serviceability. *J. Eng. Des.* **2004**, *15*, 69–90. [CrossRef]
68. Liu, S.; Yung, K.L.; Ip, W.H. Genetic local search for resource-constrained project scheduling under uncertainty. *Int. J. Inf. Manag. Sci.* **2007**, *347*–363.
69. Sanguesa, J.A.; Torres-Sanz, V.; Garrido, P.; Martinez, F.J.; Marquez-Barja, J.M. A review on electric vehicles: Technologies and challenges. *Smart Cities* **2021**, *4*, 22. [CrossRef]
70. Kondo, Y.; Deguchi, K.; Hayashi, Y.; Obata, F. Reversibility and disassembly time of part connection. *Resour. Conserv. Recycl.* **2003**, *38*, 175–184. [CrossRef]
71. Eucar. Battery Requirements for Future Automotive Applications. 2019. Available online: <https://eucar.be/wp-content/uploads/2019/08/20190710-EG-BEV-FCEV-Battery-requirements-FINAL.pdf> (accessed on 31 March 2022).

72. Prochazka, P.; Cervinka, D.; Martis, J.; Cipin, R.; Vorel, P. Li-ion battery deep discharge degradation. *ECS Trans.* **2016**, *74*, 31–36. [CrossRef]
73. Kampker, A.; Wessel, S.; Fiedler, F.; Maltoni, F. Battery pack remanufacturing process up to cell level with sorting and repurposing of battery cells. *J. Remanuf.* **2021**, *11*, 1–23. [CrossRef]
74. Bhowmick, S. Tesla Model S Battery System: An Engineer's Perspective. 2021. Available online: <https://circuitdigest.com/article/tesla-model-s-battery-system-an-engineers-perspective> (accessed on 9 May 2022).
75. Volkswagen, A.G. Long Range and Rapid Charging: The Battery System Is at the Heart of the VOLKSWAGEN ID.3, ID.4 and ID.4 GTX. 2021. Available online: <https://www.volkswagenag.com/en/news/2021/05/long-range-and-rapid-charging.html#> (accessed on 9 May 2022).
76. Das, A.; Li, D.; Williams, D.; Greenwood, D. Joining technologies for automotive battery systems manufacturing. *World Electr. Veh. J.* **2018**, *9*, 22. [CrossRef]
77. Arnberger, A.; Coskun, E.; Rutrecht, B. Recycling von lithium-ionen batterien. In *Recycling und Rohstoffe*; Thiel, S., Thomé-Kozmiensky, E., Goldmann, D., Eds.; Thomé-Kozmiensky Verlag GmbH: Neuruppin, Germany, 2018; pp. 584–599.
78. Schwarz, T.E.; Rübenauber, W.; Rutrecht, B.; Pomberger, R. Forecasting real disassembly time of industrial batteries based on virtual MTM-UAS data. *Procedia CIRP* **2018**, *69*, 927–931. [CrossRef]
79. Rohr, S.; Wagner, S.; Baumann, M.; Müller, S.; Lienkamp, M. A techno-economic analysis of end of life value chains for lithium-ion batteries from electric vehicles. In Proceedings of the 2017 Twelfth International Conference on Ecological Vehicles and Renewable Energies (EVER), Monte-Carlo, Monaco, 11–13 April 2017; pp. 1–14.
80. Hartmann, S.; Briskorn, D. An updated survey of variants and extensions of the resource-constrained project scheduling problem. *Eur. J. Oper. Res.* **2022**, *297*, 1–14. [CrossRef]
81. Herroelen, W.; Leus, R. Project scheduling under uncertainty: Survey and research potentials. *Eur. J. Oper. Res.* **2005**, *165*, 289–306. [CrossRef]
82. Slama, I.; Ben-Ammar, O.; Masmoudi, F.; Dolgui, A. Disassembly scheduling problem: Literature review and future research directions. *IFAC-Pap. OnLine* **2019**, *52*, 601–606. [CrossRef]
83. Wang, H.; Peng QZhang, J.; Gu, P. Selective disassembly planning for the end-of-life product. *Procedia CIRP* **2017**, *60*, 512–517. [CrossRef]
84. *Glocalized Solutions for Sustainability in Manufacturing. Proceedings of the 18th CIRP International Conference on Life Cycle Engineering, Technische Universität Braunschweig, Braunschweig, Germany, 2–4 May 2011*; Hesselbach, J. Ed.; Springer: Berlin/Heidelberg, Germany, 2011.
85. Hjorth, S.; Chrysostomou, D. Human–robot collaboration in industrial environments: A literature review on non-destructive disassembly. *Robot. Comput.-Integr. Manuf.* **2022**, *73*, 102208. [CrossRef]
86. Arbeitsschutzausschüsse beim BMAS. Technische Regel für Arbeitsstätten-Pausen- und Bereitschaftsräume: ASR A4.2. 2022. Available online: <https://www.baua.de/DE/Angebote/Rechtstexte-und-Technische-Regeln/Regelwerk/ASR/ASR-A4-2.html> (accessed on 15 May 2022).
87. Arbeitsschutzausschüsse beim BMAS. Technische Regel für Arbeitsstätten-Raumabmessungen und Bewegungsflächen: ASR A1.2. 2022. Available online: <https://www.baua.de/DE/Angebote/Rechtstexte-und-Technische-Regeln/Regelwerk/ASR/ASR-A1-2.html> (accessed on 15 May 2022).
88. Arbeitsschutzausschüsse beim BMAS. Technische Regel für Arbeitsstätten-Sanitärräume: ASR A4.1. 2022. Available online: <https://www.baua.de/DE/Angebote/Rechtstexte-und-Technische-Regeln/Regelwerk/ASR/ASR-A4-1.html> (accessed on 15 May 2022).
89. Arbeitsschutzausschüsse beim BMAS. Technische Regel für Arbeitsstätten-Verkehrswege: ASR A1.8. 2022. Available online: <https://www.baua.de/DE/Angebote/Rechtstexte-und-Technische-Regeln/Regelwerk/ASR/ASR-A1-8.html> (accessed on 15 May 2022).
90. *Deutsche Fassung EN 15221-6:2011; Facility Management-Teil 6: Flächenbemessung im Facility Management*. Beuth Verlag GmbH: Berlin, Germany, 2011.
91. *DIN 277; Grundflächen und Rauminhalte im Hochbau*. Beuth Verlag GmbH: Berlin, Germany, 2021.
92. Buckley, J.J.; Eslami, E. An introduction to fuzzy logic and fuzzy sets: With 14 tables. In *Advances in Soft Computing*; Physica-Verlag: Heidelberg, Germany, 2002.
93. Zadeh, L.A. Fuzzy logic. *Computer* **1988**, *21*, 83–93. [CrossRef]
94. Zhang, H.-C.; Huang, S.H. A fuzzy approach to process plan selection. *Int. J. Prod. Res.* **1994**, *32*, 1265–1279. [CrossRef]
95. Lai, Y.-J. Fuzzy mathematical programming: Methods and applications. In *Springer eBook Collection*; Springer: Berlin/Heidelberg, Germany, 1992; Volume 394.
96. Santo Pedro, F.; Carvalho de Barros, L.; Takata Gomes, L. A Survey on Fuzzy Differences. In Proceedings of the 2015 Conference of the International Fuzzy Systems Association and the European Society for Fuzzy Logic and Technology, Gijón, Spain, 30 June–3 July 2015; Atlantis Press: Paris, France, 2015.
97. Zand, M.; Nasab, M.A.; Hatami, A.; Kargar, M.; Chamorro, H.R. Using adaptive fuzzy logic for intelligent energy management in hybrid vehicles. In Proceedings of the 2020 28th Iranian Conference on Electrical Engineering (ICEE), Tabriz, Iran, 4–6 August 2020; pp. 1–7.
98. Cetin, M.S.; Guler, H.; Gencoglu, M.T. Fuzzy logic based battery control system design for electric vehicles. In Proceedings of the 2021 Innovations in Intelligent Systems and Applications Conference (ASYU), Elazig, Turkey, 6–8 October 2021; pp. 1–4.
99. Pamucar, D.; Ebadi Torkayesh, A.; Devenci, M.; Simic, V. Recovery center selection for end-of-life automotive lithium-ion batteries using an integrated fuzzy WASPAS approach. *Expert Syst. Appl.* **2022**, *206*, 117827. [CrossRef]